International Journal of Network Dynamics and Intelligence Scilight

Article

Finite-Time Bounded State Estimation for Time-Varying Systems Over FlexRay Networks With Probabilistic Bit Flips

Hongli Ge [1,2], Lei Zou [1,2,*], Hongwei Chen [1,2], and Jiyue Guo [3]

[1] College of Information Science and Technology, Donghua University, Shanghai 201620, China
[2] Engineering Research Center of Digitalized Textile and Fashion Technology, Ministry of Education, Shanghai 201620, China
[3] College of Electrical Engineering and Automation, Shandong University of Science and Technology, Qingdao 266590, China
[*] Correspondence: zouleicup@gmail.com

Received: 3 April 2025
Accepted: 26 May 2025
Published: 13 November 2025

Abstract: This paper investigates the finite-time bounded state estimation problem for time-varying systems with energy-bounded noise over communication networks. Signal transmissions over networks are subject to encoding-decoding mechanisms and probabilistic bit flips. Furthermore, the FlexRay protocol (FRP) is utilized to schedule signal transmissions, mitigating communication delays and enhancing data exchange flexibility. The objective of this article is to develop a time-varying state estimator, accounting for FRP, encoding-decoding processes, and bit errors, to ensure the desired finite-time boundedness performance. Certain time-dependent sufficient conditions are established to guarantee the required estimation performance. The desired time-varying estimator parameter is subsequently calculated by solving a recursive matrix inequality. Finally, illustrative numerical examples is presented to validate the proposed state estimation algorithm.

Keywords: FlexRay protocol; probabilistic bit flips; finite-time boundedness; time-varying systems; state estimation.

1. Introduction

With the development of network technologies, networked systems have shown a number of advantages in practical applications, including flexible architecture, easy installation, and low maintenance costs. Networked systems facilitate data exchange among various components via shared communication networks, in contrast to conventional systems, thereby providing capabilities like real-time performance and flexibility. Consequently, networked systems have garnered considerable attention from researchers. However, due to the limited communication capacity and bandwidth availability, phenomena such as data collisions, communication delays [1–4], and communication errors are inevitable. These issues present significant challenges to achieving dependable and rapid signal transmissions in wireless digital communication channels [5].

As a matter of fact, employing communication protocols is an efficient method for mitigating data collisions and communication delays. In networked systems, communication protocols define the format, mode, and rules of data transmission, thereby facilitating interpretability among diverse devices and systems through standardized communication. This standardization enhances the reliability, security, and efficiency of data transmission. In past decades, time-triggered protocols such as the well-known round-robin protocol (RRP) and stochastic communication protocol (SCP), as well as event-triggered protocols (e.g. try-once-discard protocol (TODP)), have been subjects of extensive research, see in Ref. [6–11]. For example, Ref. [8] combines the event-triggered mechanism (ETM) with finite-time control to propose a control method for fractional-order time-delay interconnected systems, successfully ensuring the dissipative performance and stability of the system. Ref. [9] proposes an analysis of finite-time

stability and a control strategy based on the event-triggered mechanism to address the security control issue of networked control systems under Denial-of-Service (DoS) attacks. Recently, a hybrid-triggered communication strategy, namely the FlexRay protocol (FRP), has recently garnered significant attention within the research community [4]. For instance, in Ref. [12], the FRP has been introduced in high-rate networks to study the finite-horizon H_∞ filtering problem of discrete-time nonlinear systems. In Ref. [13], the problem of ultimately bounded PID control for T-S fuzzy systems has been discussed under FlexRay communication protocol. The related literature is organized and presented in Table 1 for the reader's convenience. Furthermore, the research presented in Ref. [14] investigates the filter design problem for two-dimensional systems, considering the FRP and hybrid network attacks.

Table 1 Comparison of ETM and FRP-Based Approaches in the Relevant References

References	Research Problem	Main Methods
[4]	State estimation for time-varying systems with non-Gaussian noise over a FlexRay network	Recursive set-membership filtering state estimation
[8]	Control of fractional-order time-delay interconnected systems	Combination of ETM and finite-time control
[9]	Network security issues of DoS attacks	ETM-based finite-time stability and control strategy
[12]	Finite-time H_∞ filtering for discrete-time nonlinear systems via a high-rate network with FRP	Finite-time H_∞ filtering
[13]	PID control problem for T-S fuzzy systems under FRP	PID control
[14]	Filter design for two-dimensional systems with FRP and hybrid cyber attacks	Recursive set-membership filtering

It is worth noting that most of the existing research related to the FRP primarily focuses on filtering or closed-loop control problems for linear time-varying systems, nonlinear time-varying systems, or fuzzy systems affected by noise interference and network attacks, without addressing the impact of the encoding-decoding process in FRP-based network communication. Therefore, in order to fill this research gap and inspired by existing studies, this paper investigates the networked system problem of discrete-time systems affected by energy-bounded noise, considering the combined effects of the encoding-decoding process and the FlexRay scheduling protocol during data transmission.

On the other hand, in complex real-world network environments, networked systems are subject to errors during the encoding and decoding processes due to various factors. Among these, bit flips represent a significant potential issue that can substantially impact the encoding and decoding processes, especially during data transmission and storage. However, in quantization-based encoding and decoding schemes, the existing researches often assume that quantized data is amenable to error-free transmission via digital channels. However, the presence of channel noise, signal attenuation and equipment failures [15–18] invalidates this assumption. This is particularly true in widely used binary encoding schemes [19–21], where the quantized data is transmitted as a binary bit stream through symmetric channels. In such cases, channel noise can randomly cause bit flips, leading to communication errors [22]. It has been well recognized that channel noise not only induces quantization error but also results in bit error during communication. Therefore, it is vital important to consider the impact of probabilistic bit flips on data transmission.

When considering channel noise and bit errors occurring in communication networks, another challenge faced by networked systems based on the FRP is how to design the state estimator. An important issue then arises for the networked systems: how to develop an appropriate estimation strategy based on the characteristics of the influencing factors. To date, some interesting filtering algorithms have been designed in the literature which include, but are not limited to, Kalman filters [23–26], extended Kalman filters [27,28], particle filters [29], H_∞ filters [30–32], set-membership filters [4,14,33,34], and others. Compared to Kalman filtering, H_∞ filtering methods, and set-membership filtering approaches, finite-time bounded estimation methods focus on estimation performance within a finite time interval, offering lower computational complexity as well as stronger real-time performance and robustness.

Based on the above discussion, the objective of this paper is to study the finite-time bounded (FTB) state estimation problem for discrete-time varying systems subject to energy-bounded noise disturbances under the FRP and probabilistic bit flips. This problem presents three main challenges: 1) how to define the mathematical description of the switching rules between the two scheduling protocols, RRP and TODP; 2) considering the impact of probabilistic bit flips, how to represent the estimator's inputs in a unified form using time-triggered and event-triggered scheduling strategies; and 3) how to design an estimator that ensures bounded error under the influence of FRP and random probabilistic bit flips. To address these challenges, the primary technical contribution of this article can be listed as follows.

1) We propose a novel approach to address the state estimation problem in networked systems subject to energy-bounded noise disturbances, while considering the effects of probabilistic bit flips and the FlexRay scheduling protocol. This approach fills a gap in the current literature, as such combined effects have not been explored in the context of FlexRay communication systems.

2) A new estimator framework is developed that considers the joint impact of probabilistic bit flips and the

FlexRay protocol, providing a more robust and efficient solution for real-time applications.

3) The sufficient conditions for ensuring the finite-time boundedness of the estimation error are derived, providing a practical approach that system designers can implement in real-world systems.

The structure of the paper is as follows: In Section 2, we present a detailed introduction to the model used in our study, including the system under consideration, FRP, communication networks with encoding-decoding mechanism, and the encoding/decoding process under probabilistic bit flips. Then, a new measurement model is presented using lifting techniques and vector augmentation methods to describe the effects of FRP and bit flips. In Section 3, a sufficient condition for ensuring bounded estimation errors is given, along with a recursive linear matrix inequality (LMI) to solve for the estimator parameters. Section 4 presents two simulation examples to validate the correctness and scalability of the research findings. Section 5 concludes and summarizes the paper.

Notation: In this paper, $\mathbb{R}^n$ denotes the n-dimensional Euclidean space, $\mathbb{R}^{m\times n}$ represents the set of all $m\times n$ real-valued matrices, and $\mathbb{N}^+$ refers to the set of all positive integers. For a matrix P, P^{T} and P^{-1} denote its transpose and inverse, respectively. I represents the identity matrix of the appropriate dimension. For symmetric matrices X and Y, the notation $X \geqslant Y$ $(X > Y)$ indicates that $X-Y$ is positive semi-definite (positive definite). $\mathrm{diag}\{A_1, A_2, \cdots, A_n\}$ represents a block diagonal matrix whose diagonal elements are the matrices $A_1, A_2, \cdots, A_n$. $|\cdot|$ denotes the absolute value. $\mathbb{E}\{\cdot\}$, $\mathbb{P}\{\cdot\}$, and $\mathrm{Var}\{\cdot\}$ denote the expectation, probability, and variance of a random variable, respectively. $\delta(a)$ represents the Dirac delta function, which is defined as $\delta(a)=1$ when $a=0$, and $\delta(a)=0$ otherwise. $\mathrm{mod}(a,b)$ represents the remainder when the integer a is divided by the positive integer b. I denotes the identity matrix of appropriate dimension, and $\mathrm{col}\{\cdot\}$ represents a column vector.

2. Problem Formulation

2.1. System Description

In this paper, we consider the following class of discrete linear time-varying:

$$\begin{cases} x\left(T_{\varsigma+1}\right) = A\left(T_\varsigma\right) x\left(T_\varsigma\right) + B\left(T_\varsigma\right) w\left(T_\varsigma\right) \\ y\left(T_\varsigma\right) = C\left(T_\varsigma\right) x\left(T_\varsigma\right) + D\left(T_\varsigma\right) v\left(T_\varsigma\right) \end{cases} \tag{1}$$

where $x\left(T_\varsigma\right) \in \mathbb{R}^n$, $y\left(T_\varsigma\right) \in \mathbb{R}^m$, and $z\left(T_\varsigma\right) \in \mathbb{R}^p$ refer to, respectively, the system state, the measurement output measured by m sensors and the signal to be estimated; $A\left(T_\varsigma\right)$, $B\left(T_\varsigma\right)$, $C\left(T_\varsigma\right)$, and $D\left(T_\varsigma\right)$ are time-varying matrices and have the appropriate dimensions; $w\left(T_\varsigma\right) \in \mathbb{R}^w$ and $v\left(T_\varsigma\right) \in \mathbb{R}^v$ represent energy-bounded noises. We define $C\left(T_\varsigma\right) \triangleq \left[C_1^{\mathrm{T}}\left(T_\varsigma\right), C_2^{\mathrm{T}}\left(T_\varsigma\right) \cdots C_m^{\mathrm{T}}\left(T_\varsigma\right)\right]^{\mathrm{T}}$, $D\left(T_\varsigma\right) \triangleq \left[D_1^{\mathrm{T}}\left(T_\varsigma\right) D_2^{\mathrm{T}}\left(T_\varsigma\right) \cdots D_m^{\mathrm{T}}\left(T_\varsigma\right)\right]^{\mathrm{T}}$ and $h \triangleq T_{\varsigma+1} - T_\varsigma$, where T_ς represents the sampling time, $\varsigma \in \{0, 1, \cdots, N\}$ and $N \in \mathbb{N}^+$. Actually, h means the time interval or evolution period of the target system.

2.2. FlexRay Transmission Scheduling Protocol

Due to bandwidth limitations in network transmission, it is of great significance to adopt appropriate communication protocols to regulate data transmission on shared channels. As shown in Figure 1, we introduce FRP to schedule data from the encoder to the state estimator via the transmission network, aiming to achieve flexibility and reliability in data transmission.

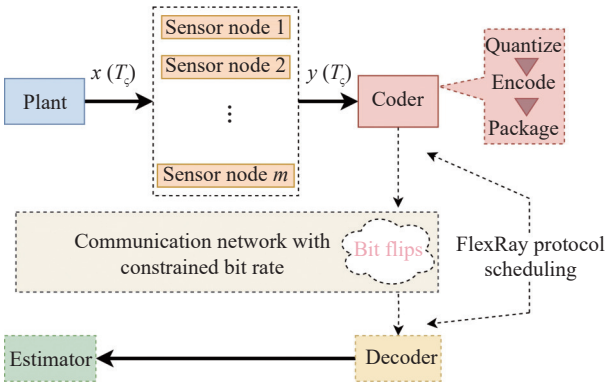

Figure 1. Framework for the FlexRay network under bit flips.

As described by Figure 2, each communication cycle in a FlexRay network consists of four segments: the static segment, the dynamic segment, the symbol window, and the network idle time. The time durations of the symbol

window and the network idle time are relatively short compared to those of the first two segments, and are therefore often neglected in theoretical research. Assuming the time durations of these four segments are $S1$, $S2$, $S3$, and $S4$, respectively. It is easy to obtain $S3 = S4 = 0$. Furthermore, we assume that $S1 = lh$, $(l \in \mathbb{N})$ and $S2 = h$. Then, the time duration of one communication cycle is $S1 + S2 + S3 + S4 = (l+1)h = fh$. In the following, we will provide a detailed introduction to the scheduling principles of the FRP.

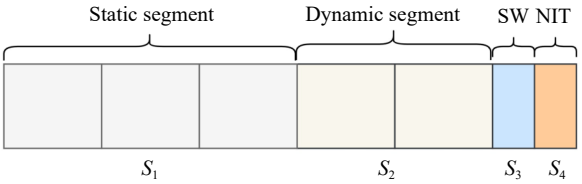

Figure 2. A communication cycle of the FlexRay network.

In this paper, data transmission in the static segment and dynamic segment follows two different communication protocols. In the static segment, scheduling adheres to the RRP, while in the dynamic segment, scheduling follows the TODP. Suppose that m nodes are divided into $\mathcal{I}_1 \triangleq \{1,2,\cdots,l\}$ and $\mathcal{I}_2 \triangleq \{l+1,l+2,\cdots,m\}$ two parts, where the output data of the nodes in the first part are transmitted in the static segment, and the output data of the nodes in the second part are transmitted in the dynamic segment.

Let

$$\begin{aligned}
y\left(T_\varsigma\right) &\triangleq \left[\left(y^{(1)}\left(T_\varsigma\right)\right)^{\mathrm{T}} \quad \left(y^{(2)}\left(T_\varsigma\right)\right)^{\mathrm{T}}\right]^{\mathrm{T}},\\
\bar{y}\left(T_\varsigma\right) &\triangleq \left[\left(\bar{y}^{(1)}\left(T_\varsigma\right)\right)^{\mathrm{T}} \quad \left(\bar{y}^{(2)}\left(T_\varsigma\right)\right)^{\mathrm{T}}\right]^{\mathrm{T}},\\
y^{(1)}\left(T_\varsigma\right) &\triangleq \left[y_1\left(T_\varsigma\right) \quad \cdots \quad y_l\left(T_\varsigma\right)\right]^{\mathrm{T}},\\
y^{(2)}\left(T_\varsigma\right) &\triangleq \left[y_{l+1}\left(T_\varsigma\right) \quad \cdots \quad y_m\left(T_\varsigma\right)\right]^{\mathrm{T}},\\
\bar{y}^{(1)}\left(T_\varsigma\right) &\triangleq \left[\bar{y}_1\left(T_\varsigma\right) \quad \cdots \quad \bar{y}_l\left(T_\varsigma\right)\right]^{\mathrm{T}},\\
\bar{y}^{(2)}\left(T_\varsigma\right) &\triangleq \left[\bar{y}_{l+1}\left(T_\varsigma\right) \quad \cdots \quad \bar{y}_m\left(T_\varsigma\right)\right]^{\mathrm{T}},
\end{aligned}$$

where $y^{(1)}\left(T_\varsigma\right)$ representing the first l components of the measurement output $y\left(T_\varsigma\right)$ will be transmitted via the network after being scheduled by RRP; $y^{(2)}\left(T_\varsigma\right)$ are the m-l components of $y\left(T_\varsigma\right)$, which will be scheduled by TODP. $\bar{y}^{(1)}(T_\varsigma)$ represents the measurement values after network transmission scheduled by the RRP, which corresponds to the first l components of the measurement output $\bar{y}(T_\varsigma)$ after transmission. $\bar{y}^{(2)}(T_\varsigma)$ represents the measurement values after network transmission scheduled by the TODP, corresponding to the remaining $m-l$ components of $\bar{y}(T_\varsigma)$ after transmission.

The RRP is a scheduling method that allocates fixed time slots to each node in a cyclic order, ensuring equal access to the network for all nodes. This protocol is commonly used in real-time and time-sensitive applications, such as communication systems and IoT networks, where fairness in data transmission is crucial. However, if some nodes have less data to transmit, RRP may lead to higher latency and inefficiency. On the other hand, the TODP allows nodes to transmit data once, and if the transmission fails, the data is discarded. This helps reduce network congestion and latency. In the context of FRP, it effectively combines the advantages of both of the above protocols. The following outlines the principles for selecting sensor nodes using these two protocols.

1) RRP: Data transmission in the static segment is scheduled by the static communication protocol, namely, the well-known RRP. At time T_ς, the principle for gating the sensor node under this protocol is as follows:

$$\lambda_{T_\varsigma} \triangleq \mathrm{mod}\left(T_\varsigma, l\right) + 1 \tag{2}$$

where $\lambda_{T_\varsigma} \in \mathcal{I}_1 \triangleq \{1,\cdots,l\}$ stands for the node using the communication network at instant T_ς. Note that only the component $y_{\lambda_{T_\varsigma}}\left(T_\varsigma\right)$ within $y^{(1)}\left(T_\varsigma\right)$ undergoes an update, whereas the remaining components of $y^{(1)}\left(T_\varsigma\right)$ are zeroed out using the zero-input strategy.

2) TODP: Data transmission in the dynamic segment is scheduled by the dynamic communication protocol, namely, the so-called TODP. At time T_ς, the principle for gating the sensor node under this protocol is as follows:

$$\alpha_{T_\varsigma} \triangleq \max_{i=l+1,\cdots,m} \left\{\left(\tilde{y}_i^{(2)}\left(T_\varsigma\right)\right)^{\mathrm{T}} \Omega_i\left(T_\varsigma\right) \tilde{y}_i^{(2)}\left(T_\varsigma\right)\right\} \tag{3}$$

where $\alpha_{T_\varsigma} \in \mathcal{I}_2 \triangleq \{l+1,\cdots,m\}$ is the node qualified to enter the transmission network at the current time;

$\Omega_i\left(T_\varsigma\right)\left(i\in\mathcal{I}_2\right)$ are given weighted matrices; and $\tilde{y}_i^{(2)}\left(T_\varsigma\right)\triangleq y_i^{(2)}\left(T_\varsigma\right)-\bar{y}_i^{(2)}\left(T_{\varsigma-1}\right)$. By using the zero-order-holder strategy, $\bar{y}_i\left(T_\varsigma\right)\left(i\in\mathcal{I}_2\right)$ can be expressed by

$$\bar{y}_i\left(T_\varsigma\right)=\begin{cases}y_i\left(T_\varsigma\right), & \text{if } i=\alpha_{T_\varsigma}\\ \bar{y}_i\left(T_{\varsigma-1}\right) & \text{otherwise.}\end{cases} \tag{4}$$

Remark 1: In theoretical studies, since symbol windows and network idle times are primarily dedicated to network management and synchronization, their direct influence on data transmission efficiency and network performance is relatively minor, hence they are often overlooked. Additionally, considering that the FlexRay Protocol is typically utilized for intra-vehicle data communication, characterized by short transmission distances and high transmission rates, the data packet transmission time is negligible relative to the comprehensive communication cycle and, consequently, may be disregarded. In conclusion, to streamline the analysis and emphasize the key factors, this paper omits the specific impacts of symbol window duration, network idle time, and data transmission time in the course of the research.

2.3. Description of Quantization Effects in the Network

In practical digital communication networks, the original signal from the sensor must first undergo quantization and then be encoded into binary characters for transmission by an encoder. To adapt to digital communication methods, this paper employs a uniform quantizer, which divides the value range of the sensor measurement signal into equal intervals. The quantization process involves mapping these intervals to discrete output values.

Without loss of generality, assume that for the quantizer at node i, with a given positive scalar $\sigma_i>0$, the measurement for the i-th sensor satisfies the following constraint

$$\left|y_i(T_\varsigma)\right|\leqslant\sigma_i. \tag{5}$$

where $y_i(T_\varsigma)$ is the i-th element of the vector $y(T_\varsigma)$.

By choosing an integer Δ_i as the quantization level, i.e., the number of region intervals, the quantization region can be uniformly divided into several sub-intervals, which can be denoted by

$$\begin{cases}\mathcal{Q}_{1,i}:-\sigma_i\leqslant y_i(T_\varsigma)<-\sigma_i+\frac{2\sigma_i}{\Delta_i}\\ \mathcal{Q}_{2,i}:-\sigma_i+\frac{2\sigma_i}{\Delta_i}\leqslant y_i(T_\varsigma)<-\sigma_i+\frac{4\sigma_i}{\Delta_i}\\ \quad\vdots\\ \mathcal{Q}_{\Delta_i,i}:\sigma_i-\frac{2\sigma_i}{\Delta_i}\leqslant y_i(T_\varsigma)\leqslant\sigma_i.\end{cases} \tag{6}$$

To ensure that the information within each sub-interval is uniquely encoded, assume that the maximum quantization level corresponding to the i-th quantizer is $\widetilde{\Delta}_i\triangleq 2^{\Lambda_i}$, where $i\in\mathcal{I}\triangleq\{1,2,\cdots,m\}$ and Λ_i is the bit rate corresponding to node i.

Let the corresponding quantization region for m sensors be $\{s_1,s_2,\cdots,s_m\}$, $s_i\in\{1,2,\cdots,\Delta_i\}$. We approximate the original data by taking the central value of each subinterval, and the calculation formula can be denoted by

$$q\left(y_i(T_\varsigma)\right)=-\sigma_i+\frac{(2s_i-1)\sigma_i}{\widetilde{\Delta}_i}. \tag{7}$$

According to the above analysis and description, the quantization error corresponding to the measurement value of the i-th sensor is defined as:

$$\varphi_i(T_\varsigma)\triangleq y_i(T_\varsigma)-q\left(y_i(T_\varsigma)\right) \tag{8}$$

furthermore, from (6) and (7), it can be inferred that the maximum quantization error is equivalent to the distance from the center point of the subinterval to the endpoint of this interval. Therefore, the absolute value of the quantization error of the measurement value satisfies the following inequality:

$$\left|\varphi_i(T_\varsigma)\right|\leqslant\frac{\sigma_i}{\widetilde{\Delta}_i}. \tag{9}$$

Remark 2: In digital communication networks, quantization is the process of transforming continuous signals into discrete signals. Commonly employed quantization methods include uniform quantization and non-uniform quantization. Uniform quantization is a method that divides the dynamic range of the input signal into several equal intervals. Within each interval, the signal value is mapped to the midpoint of that interval. Since all the quantization intervals are of the same size, uniform quantization is relatively simple and efficient to implement, making it suitable

for general signal transmission. Non-uniform quantization, on the other hand, divides the signals dynamic range into intervals of different sizes, with the interval sizes adjusted according to the characteristics of the signal. This method involves higher computational complexity. Consequently, to enhance coding efficiency and conserve computational resources, this study employs uniform quantization for data discretization.

2.4. Encoding-Decoding Process and Probabilistic Bit Flips

As illustrated in Figure 1, sensor measurement data first undergoes quantization processing by a quantizer, followed by conversion into a binary data stream by an encoder. This data stream is then transmitted over a digital communication network. However, during actual transmission, various factors such as noise interference and equipment failures often result in significant bit errors, known as bit flips, which have a notable impact on decoding accuracy. Regrettably, many studies overlook this crucial aspect, leading to overly idealized research results.

To conduct a more detailed analysis of the impact of bit flips on network data transmission and estimation performance, we first introduce a relevant mathematical model [16]. Assume that the bit rate corresponding to node i is Λ_i. For node i, the uniformly quantized output in (7) is mapped to one of the Δ_i discrete values, which are represented as integers $\{0,1,2,\cdots,\Delta_i-1\}$, meaning that each quantized value is associated with an integer index. Therefore, the i-th encoder converts each quantized integer value $\bar{s}_i \in \{0,1,2,\cdots,\Delta_i-1\}$ into a binary stream, as expressed in the following form:

$$\mathcal{D}_i(T_\varsigma) \triangleq \left\{\theta_{i,1}(T_\varsigma),\theta_{i,2}(T_\varsigma),\cdots,\theta_{i,\Lambda_i}(T_\varsigma)\right\} \tag{10}$$

where $\theta_{i,r}(T_\varsigma) \in \{0,1\}$ denotes the codeword corresponding to the encoded data from the i-th sensor and $r \in \{1,2,\cdots,\Lambda_i\}$ represents the number of bits.

The quantization output (7) is further expressed in the following form using concrete bits

$$q\left(y_i(T_\varsigma)\right) = -\sigma_i + \frac{\left(2\sum_{r=1}^{\Lambda_i}\theta_{i,r}(T_\varsigma)2^{r-1}+1\right)\sigma_i}{\widetilde{\Delta}_i}. \tag{11}$$

Assuming that the probability of a bit flip occurring at the r-th bit of the data from the i-th encoder follows a Bernoulli distribution, denoted as $\rho_{i,r}$, we can deduce that

$$\rho_{i,r}(T_\varsigma) = \begin{cases} 1, & \text{the } r\text{−th bit is flipped} \\ 0, & \text{the } r\text{−th bit remains unchanged.} \end{cases} \tag{12}$$

Considering the bit flips that occur with the aforementioned probability, the resulting codeword can be represented as

$$\check{\theta}_{i,r}(T_\varsigma) = \rho_{i,r}(T_\varsigma)\left(1-\theta_{i,r}(T_\varsigma)\right) + \left(1-\rho_{i,r}(T_\varsigma)\right)\theta_{i,r}(T_\varsigma) \tag{13}$$

where $\check{\theta}_{i,r}(T_\varsigma) \in \{0,1\}$, representing the codeword of the r-th bit for the i-th coder data. Therefore the data received by decoder i from the bitstream can be further expressed as

$$\check{\mathcal{D}}_i(T_\varsigma) \triangleq \left\{\check{\theta}_{i,1}(T_\varsigma),\check{\theta}_{i,2}(T_\varsigma),\cdots,\check{\theta}_{i,\Lambda_i}(T_\varsigma)\right\}. \tag{14}$$

For the purpose of analysis, we postulate that the flipping of each bit occurs independently of one another and adheres to

$$\mathbb{P}\left\{\rho_{i,r}(T_\varsigma)=1\right\} = \bar{\rho}_i \tag{15}$$

where $\bar{\rho}_i \in (0,1)$ for $i \in \mathcal{I}$ is a known constant.

Accordingly, following its journey through the wireless digital network and encountering probabilistic bit flipping, the resultant decoded output is further expressed as

$$\check{q}\left(y_i(T_\varsigma)\right) = -\sigma_i + \frac{\left(2\sum_{r=1}^{\Lambda_i}\check{\theta}_{i,r}(T_\varsigma)2^{r-1}+1\right)\sigma_i}{\widetilde{\Delta}_i}. \tag{16}$$

For the convenience of subsequent analysis and comprehension, let $\varphi\left(T_\varsigma\right) \triangleq \left[\varphi_1^{\mathrm{T}}\left(T_\varsigma\right),\varphi_2^{\mathrm{T}}\left(T_\varsigma\right),\cdots,\varphi_m^{\mathrm{T}}\left(T_\varsigma\right)\right]^{\mathrm{T}}$, $\vec{y}_i(T_\varsigma) \triangleq q\left(y_i(T_\varsigma)\right)$ and $\check{\mathrm{y}}_{\mathrm{i}}\left(T_\varsigma\right) \triangleq \check{q}\left(y_i(T_\varsigma)\right)$, then the quantized measurement output and the decoding measurement output can be denoted as

$$\vec{y}(T_\varsigma) \triangleq \left[\left(\vec{y}^{(1)}\left(T_\varsigma\right)\right)^{\mathrm{T}} \quad \left(\vec{y}^{(2)}\left(T_\varsigma\right)\right)^{\mathrm{T}}\right]^{\mathrm{T}} \tag{17}$$

and

$$\check{y}\left(T_\varsigma\right) \triangleq \left[\left(\check{y}^{(1)}\left(T_\varsigma\right)\right)^{\mathrm{T}} \quad \left(\check{y}^{(2)}\left(T_\varsigma\right)\right)^{\mathrm{T}}\right]^{\mathrm{T}} \tag{18}$$

where

$$\begin{aligned}
\vec{y}^{(1)}\left(T_\varsigma\right) &\triangleq \left[\vec{y}_1\left(T_\varsigma\right) \quad \cdots \quad \vec{y}_l\left(T_\varsigma\right)\right]^{\mathrm{T}}, \\
\vec{y}^{(2)}\left(T_\varsigma\right) &\triangleq \left[\vec{y}_{l+1}\left(T_\varsigma\right) \quad \cdots \quad \vec{y}_m\left(T_\varsigma\right)\right]^{\mathrm{T}}, \\
\check{y}^{(1)}\left(T_\varsigma\right) &\triangleq \left[\check{y}_1\left(T_\varsigma\right) \quad \cdots \quad \check{y}_l\left(T_\varsigma\right)\right]^{\mathrm{T}}, \\
\check{y}^{(2)}\left(T_\varsigma\right) &\triangleq \left[\check{y}_{l+1}\left(T_\varsigma\right) \quad \cdots \quad \check{y}_m\left(T_\varsigma\right)\right]^{\mathrm{T}}.
\end{aligned}$$

In what follows, to handle the decoding output $\check{y}_{\mathrm{i}}\left(T_\varsigma\right)$ that contains uncertainty, a lemma is provided to characterize its statistical properties

Remark 3: In the context of binary encoding-decoding mechanisms, transmission errors primarily stem from two sources: quantization error and bit-flip error. Quantization error is influenced by the quantization interval, which can be reduced by increasing the number of bits, thereby lowering the quantization error. On the other hand, bit-flip error can be minimized by utilizing a more reliable communication channel with a lower crossover probability.

Lemma 1: [5]: Consider the signal $\vec{y}_i(T_\varsigma)$ being transmitted through a memoryless binary symmetric channel, and we denote $\bar{\rho}_i$ as the probability of a bit flip. Subsequently, the decoded signal $\check{y}_i\left(T_\varsigma\right)$ will possess a mean and variance as follows

$$\mathbb{E}\left\{\check{y}_i(T_\varsigma)\right\} = (1-2\bar{\rho}_i)\vec{y}_i(T_\varsigma) \tag{19}$$

and

$$\mathcal{D}_i \triangleq \mathrm{Var}\left\{\check{y}_i(T_\varsigma)\right\} = \frac{4}{3}\bar{\rho}_i(1-\bar{\rho}_i)\frac{\sigma_i^2\left(2^{2\Lambda_i}-1\right)}{2^{2\Lambda_i}} \tag{20}$$

where the expectation is determined based on the stochastic variables $\rho_{i,r}(T_\varsigma)$.

According to Lemma 1, the output of the decoding process is further expressed as

$$\check{y}_i(T_\varsigma) = (1-2\bar{\rho}_i)\vec{y}_i(T_\varsigma) + \mathcal{A}_i(T_\varsigma) \tag{21}$$

where $\mathcal{A}_i(T_\varsigma)$ represents a stochastic variable characterized by a zero mean and a variance of $\mathcal{D}_i$.

From (21) and the definition of $\check{y}(T_\varsigma)$, we have

$$\check{y}(T_\varsigma) = \widetilde{P}\vec{y}(T_\varsigma) + \mathcal{A}(\mathcal{T}_\varsigma) \tag{22}$$

where $\widetilde{P} \triangleq \mathrm{diag}\{1-2\bar{\rho}_1, 1-2\bar{\rho}_2, \cdots, 1-2\bar{\rho}_m\}$, $\mathcal{A}(\mathcal{T}_\varsigma) \triangleq \left[(\mathcal{A}_\infty(\mathcal{T}_\varsigma))^{\mathrm{T}} \quad (\mathcal{A}_\in(\mathcal{T}_\varsigma))^{\mathrm{T}} \quad \cdots \quad (\mathcal{A}_\Updownarrow(\mathcal{T}_\varsigma))^{\mathrm{T}}\right]^{\mathrm{T}}$.

2.5. New Measurement Model

Due to the periodic characteristics of FRP, we are interested in its impact on estimator design within a single communication cycle. To avoid the challenges posed by FRP's switching rules, we set the update period of the measurement output after network transmission $\bar{y}\left(T_\varsigma\right)$ to be the length of the communication cycle, which is fh (where f and h are constants). Similarly, the update period of the state estimator is also set to fh. Since node selection by TODP may vary, there exist $m-l$ different communication cycles. In what follows, We will adopt lifting techniques [35] to uniformly set the update period of the target plant to fh.

Lemma 2: The given plant (1) can be reformulated into the following representation:

$$\bar{x}\left(t_{\varsigma+1}\right) = \bar{\mathcal{A}}\left(t_\varsigma\right)\bar{x}\left(t_\varsigma\right) + \bar{\mathcal{B}}\left(t_\varsigma\right)\bar{w}\left(t_\varsigma\right) \tag{23}$$

where $t_0 = 0$, $t_{\varsigma+1} - t_\varsigma \triangleq (l+1)h = fh$, and

$$\bar{x}(t_\varsigma) \triangleq \begin{bmatrix} x(t_{\varsigma-1}+h) \\ x(t_{\varsigma-1}+2h) \\ \vdots \\ x(t_\varsigma) \end{bmatrix}, \ \bar{\mathcal{A}}(t_\varsigma) \triangleq \begin{bmatrix} \vec{A}_1(t_\varsigma) \\ \vec{A}_2(t_\varsigma) \\ \vdots \\ \vec{A}_f(t_\varsigma) \end{bmatrix},$$

$$\bar{\mathcal{B}}(t_\varsigma) \triangleq \begin{bmatrix} B_1^{(f)}(t_\varsigma) \\ B_2^{(f-1)}(t_\varsigma) \\ \vdots \\ B_f^{(1)}(t_\varsigma) \end{bmatrix}, \bar{w}(t_\varsigma) \triangleq \begin{bmatrix} w(t_\varsigma) \\ w(t_\varsigma + h) \\ \vdots \\ w(t_\varsigma + (f-1)h) \end{bmatrix},$$

$$\vec{A}_i(t_\varsigma) \triangleq \left\{ \underbrace{0, \cdots, 0}_{f-1}, A_i(t_\varsigma) \right\}, i = 1, \cdots, f,$$

$$A_{f-b+1}(t_\varsigma) \triangleq \prod_{i=b}^{f} A(t_{\varsigma+1} - ih), b = 1, \cdots, f,$$

$$B_b^{(r)}(t_\varsigma) \triangleq \begin{cases} \begin{bmatrix} B(t_\varsigma) & \underbrace{0 \ \cdots \ 0}_{f-1} \end{bmatrix}, b = 1, r = f \\ \begin{bmatrix} \check{B}_b^{(r)}(t_\varsigma) & B(t_\varsigma + (b-1)h) & \underbrace{0 \ \cdots \ 0}_{f-b} \end{bmatrix}, \\ b = 2, \cdots, f, r = f - b + 1 \end{cases}$$

$$\check{B}_b^{(r)} \triangleq \left[\vec{B}_1^{(r)}(t_\varsigma) \quad \cdots \quad \vec{B}_{b-1}^{(r)}(t_\varsigma) \right],$$

$$\vec{B}_j^{(r)}(t_\varsigma) \triangleq \prod_{i=r}^{f-j} A(t_{\varsigma+1} - ih) B(t_\varsigma + (j-1)h),$$

$$j = 1, \cdots, b-1.$$

Proof: Firstly, based on (1), we obtain

$$\begin{aligned} x\left(t_\varsigma + h\right) =& A\left(t_{\varsigma+1} - fh\right) x\left(t_\varsigma\right) + B\left(t_\varsigma\right) w\left(t_\varsigma\right) \\ =& A_1\left(t_\varsigma\right) x\left(t_\varsigma\right) + B_1^{(f)}\left(t_\varsigma\right) \bar{w}\left(t_\varsigma\right) \end{aligned} \tag{24}$$

and proceed further

$$\begin{aligned} x\left(t_\varsigma + 2h\right) =& A\left(t_\varsigma + h\right) x\left(t_\varsigma + h\right) + B\left(t_\varsigma + h\right) w\left(t_\varsigma + h\right) \\ =& A\left(t_\varsigma + h\right) \left(A_1\left(t_\varsigma\right) x\left(t_\varsigma\right) + B\left(t_\varsigma\right) w\left(t_\varsigma\right)\right) \\ & + B\left(t_\varsigma + h\right) w\left(t_\varsigma + h\right) \\ =& A_2\left(t_\varsigma\right) x\left(t_\varsigma\right) + B_2^{(f-1)}\left(t_\varsigma\right) \bar{w}\left(t_\varsigma\right) \end{aligned} \tag{25}$$

$$x\left(t_{\varsigma+1} - h\right) = A_{f-1}\left(t_\varsigma\right) x\left(t_\varsigma\right) + B_{f-1}^{(2)}\left(t_\varsigma\right) \bar{w}\left(t_\varsigma\right). \tag{26}$$

Consequently, we obtain

$$\begin{aligned} x\left(t_{\varsigma+1}\right) =& A\left(t_{\varsigma+1} - h\right) x\left(t_{\varsigma+1} - h\right) \\ & + B\left(t_\varsigma + (f-1)h\right) w\left(t_\varsigma + (f-1)h\right) \\ =& A\left(t_{\varsigma+1} - h\right) \left(A_{f-1}\left(t_\varsigma\right) x\left(t_\varsigma\right) + B_{f-1}^{(2)}\left(t_\varsigma\right) \bar{w}\left(t_\varsigma\right)\right) \\ & + B\left(t_\varsigma + (f-1)h\right) w\left(t_\varsigma + (f-1)h\right) \\ =& A_f\left(t_\varsigma\right) x\left(t_\varsigma\right) + B_f^{(1)}\left(t_\varsigma\right) \bar{w}\left(t_\varsigma\right). \end{aligned} \tag{27}$$

Accordingly, we derive the concise form (23), thereby concluding the proof of the lemma. ■

Under the effects of protocol-scheduling-based communication, at each transmission instant, only one sensor node will be selected to gain the access to the communication channel, consequently leading to the update of a corresponding component of the measurement output. According to such a process, we introduce the following Lemma to derive the update formula for the received measurement output $\bar{y}\left(t_\varsigma\right)$ after it has been transmitted through the network.

Lemma 3: Based on the operating principles of FRP, the received measurement output $\bar{y}\left(t_\varsigma\right)$ can be represented as

$$\begin{aligned} \bar{y}\left(t_\varsigma\right) =& \hat{C}\left(t_\varsigma\right) \bar{x}\left(t_\varsigma\right) + \check{D}\left(t_\varsigma\right) \bar{v}\left(t_\varsigma\right) \\ & + \ell_2 \left(I - \Phi_{\sigma_{t_\varsigma + lh}}\right) \bar{y}^{(2)}\left(t_{\varsigma-1}\right) \\ & + H\left(t_\varsigma\right) \eta\left(t_\varsigma\right) \end{aligned} \tag{28}$$

where

$$
\begin{aligned}
&\eta\left(t_\varsigma\right) \triangleq \left[\bar{\varphi}^{\mathrm{T}}\left(t_\varsigma\right) \quad \bar{\mathcal{A}}^{\mathrm{T}}\left(t_\varsigma\right)\right]^{\mathrm{T}},\\
&\ell_1 \triangleq \left[I_{l\times l} \quad 0^{\mathrm{T}}_{(m-l)\times l}\right]^{\mathrm{T}},\\
&\ell_2 \triangleq \left[0^{\mathrm{T}}_{l\times(m-l)} \quad I_{(m-l)\times(m-l)}\right]^{\mathrm{T}},\\
&\mathcal{I}_1 \triangleq \left[\check{\mathcal{I}}_1^{\mathrm{T}} \quad \check{\mathcal{I}}_2^{\mathrm{T}} \quad \cdots \quad \check{\mathcal{I}}_l^{\mathrm{T}}\right]^{\mathrm{T}}_{l\times(fm)},\\
&\mathcal{I}_2 \triangleq \left[0 \quad I_{(m-l)\times(m-l)}\right]^{\mathrm{T}}_{l\times(fm)},\\
&\widetilde{P}_1 \triangleq \mathrm{diag}\{1-2\bar{\rho}_1,\cdots,1-2\bar{\rho}_l\},\\
&\widetilde{P}_2 \triangleq \mathrm{diag}\{1-2\bar{\rho}_{l+1},\cdots,1-2\bar{\rho}_m\},\\
&H\left(t_\varsigma\right) \triangleq \ell_1\widetilde{H}\left(t_\varsigma\right)+\ell_2\check{H}\left(t_\varsigma\right),\\
&\bar{v}\left(t_\varsigma\right) \triangleq \mathrm{col}\left\{v\left(t_\varsigma\right)v\left(t_\varsigma+h\right),\cdots,v\left(t_\varsigma+(f-1)h\right)\right\},\\
&\bar{\varphi}\left(t_\varsigma\right) \triangleq \mathrm{col}\left\{\varphi\left(t_\varsigma\right),\varphi\left(t_\varsigma+h\right),\cdots,\varphi\left(t_\varsigma+(f-1)h\right)\right\},\\
&\bar{\mathcal{A}}(t_\varsigma) \triangleq \mathrm{col}\left\{\mathcal{A}(t_\varsigma),\mathcal{A}\left(t_\varsigma+h\right),\cdots,\mathcal{A}\left(t_\varsigma+(f-1)h\right)\right\},\\
&\widetilde{H}\left(t_\varsigma\right) \triangleq \left[-\widetilde{P}_1\mathcal{I}_1 \quad \mathcal{I}_1\right],\\
&\check{H}\left(t_\varsigma\right) \triangleq \left[-\Phi_{\sigma_{t_\varsigma+lh}}\widetilde{P}_2\mathcal{I}_2 \quad \Phi_{\sigma_{t_\varsigma+lh}}\mathcal{I}_2\right],\\
&\hat{C}\left(t_\varsigma\right) \triangleq \ell_1\tilde{C}\left(t_\varsigma\right)+\ell_2\acute{C}\left(t_\varsigma\right),\\
&\check{D}\left(t_\varsigma\right) \triangleq \ell_1\tilde{D}\left(t_\varsigma\right)+\ell_2\acute{D}\left(t_\varsigma\right),\\
&\tilde{C}\left(t_\varsigma\right) \triangleq \widetilde{P}_1\tilde{C}_1\left(t_\varsigma\right)+\widetilde{P}_1\tilde{C}_2\left(t_\varsigma\right)\bar{\mathcal{A}}\left(t_\varsigma\right),\\
&\tilde{D}\left(t_\varsigma\right) \triangleq \widetilde{P}_1\tilde{C}_2\left(t_\varsigma\right)\bar{\mathcal{B}}\left(t_\varsigma\right)+\widetilde{P}_1\tilde{D}_1\left(t_\varsigma\right),\\
&\acute{C}\left(t_\varsigma\right) \triangleq \Phi_{\sigma_{t_\varsigma+lh}}\widetilde{P}_2\check{C}\left(t_\varsigma+lh\right)\bar{\mathcal{A}}\left(t_\varsigma\right),\\
&\check{\mathcal{I}}_i \triangleq \begin{cases} \left[1 \quad \underbrace{0 \quad \cdots \quad 0}_{fm-1}\right]_{1\times(fm)}, i=1\\ \left[\underbrace{0 \quad \cdots \quad 0}_{(l-1)(m+1)} \quad 1 \quad 0 \quad \cdots \quad 0\right]_{1\times(fm)}, i=l \end{cases},\\
&\acute{D}\left(t_\varsigma\right) \triangleq \Phi_{\sigma_{t_\varsigma+lh}}\widetilde{P}_2\check{C}\left(t_\varsigma+lh\right)\bar{\mathcal{B}}\left(t_\varsigma\right)\\
&\qquad\quad +\Phi_{\sigma_{t_\varsigma+lh}}\widetilde{P}_2\check{D}\left(t_\varsigma+lh\right),\\
&\check{C}\left(t_\varsigma+lh\right) \triangleq \left[\check{C}^{\mathrm{T}}_{l+1}\left(t_\varsigma+lh\right),\cdots,\check{C}^{\mathrm{T}}_m\left(t_\varsigma+lh\right)\right],\\
&\check{D}\left(t_\varsigma+lh\right) \triangleq \left[\check{D}^{\mathrm{T}}_{l+1}\left(t_\varsigma+lh\right),\cdots,\check{D}^{\mathrm{T}}_m\left(t_\varsigma+lh\right)\right],\\
&\Phi_{\sigma_{t_\varsigma}+lh} \triangleq \mathrm{diag}\left\{\delta\left(l+1-\sigma_{t_\varsigma+lh}\right),\cdots,\delta\left(m-\sigma_{t_\varsigma+lh}\right)\right\},\\
&\check{C}_i\left(t_\varsigma+lh\right) \triangleq [\underbrace{0,\cdots,0}_{f-2},C_i\left(t_\varsigma+lh\right),0]_{1\times(fn)},\\
&\check{D}_i\left(t_\varsigma+lh\right) \triangleq [\underbrace{0,\cdots,0}_{f-1},D_i\left(t_\varsigma+lh\right)]_{l\times(fw)},\\
&\tilde{C}_1\left(t_\varsigma\right) \triangleq [\vec{C}^{\mathrm{T}}_1\left(t_\varsigma\right),\underbrace{0,\cdots,0}_{l-1}]^{\mathrm{T}}_{l\times(fn)},\\
&\tilde{C}_2\left(t_\varsigma\right) \triangleq \left[0,\vec{C}^{\mathrm{T}}_2\left(t_\varsigma+h\right),\cdots,\vec{C}^{\mathrm{T}}_l\left(t_\varsigma+(l-1)h\right)\right]^{\mathrm{T}}_{l\times(fn)},\\
&\tilde{D}_1\left(t_\varsigma\right) \triangleq \left[\vec{D}^{\mathrm{T}}_1\left(t_\varsigma+h\right),\cdots,\vec{D}^{\mathrm{T}}_l\left(t_\varsigma+(l-1)h\right)\right]^{\mathrm{T}}_{l\times(fw)},\\
&\vec{C}_1\left(t_\varsigma\right) \triangleq [\underbrace{0,\cdots,0}_{f-1},C_1\left(t_\varsigma\right)],\\
&\vec{C}_j\left(t_\varsigma+(j-1)h\right) \triangleq [\underbrace{0,\cdots,0}_{j-2},C_j\left(t_\varsigma+(j-1)h\right),\underbrace{0,\cdots,0}_{f+1-j}],\\
&\vec{D}_r\left(t_\varsigma+(r-1)h\right) \triangleq [\underbrace{0,\cdots,0}_{r-1},D_r\left(t_\varsigma+(r-1)h\right),\underbrace{0,\cdots,0}_{f-r}].
\end{aligned}
$$

Proof: Based on (1), (2) and (22), we obtain

$$\begin{aligned}\bar{y}^{(1)}\left(t_\varsigma\right) &= \check{y}^{(1)}\left(t_\varsigma\right)\\ &= \widetilde{P}_1\bar{y}^{(1)}\left(t_\varsigma\right)+\mathcal{I}_1\bar{\mathcal{A}}\left(t_\varsigma\right)\\ &= \widetilde{P}_1 y^{(1)}\left(t_\varsigma\right)-\widetilde{P}_1\mathcal{I}_1\bar{e}\left(t_\varsigma\right)+\mathcal{I}_1\bar{\mathcal{A}}\left(t_\varsigma\right)\\ &= \tilde{C}\left(t_\varsigma\right)\bar{x}\left(t_\varsigma\right)+\widetilde{D}\left(t_\varsigma\right)\bar{v}\left(t_\varsigma\right)-\widetilde{P}_1\mathcal{I}_1\bar{\varphi}\left(t_\varsigma\right)+\mathcal{I}_1\bar{\mathcal{A}}\left(t_\varsigma\right)\\ &= \tilde{C}\left(t_\varsigma\right)\bar{x}\left(t_\varsigma\right)+\widetilde{D}\left(t_\varsigma\right)\bar{v}\left(t_\varsigma\right)+\widetilde{H}\left(t_\varsigma\right)\eta\left(t_\varsigma\right).\end{aligned} \tag{29}$$

Similarly, according to (1), (3) and (22), $\bar{y}^{(2)}$ can be calculated as

$$\begin{aligned}\bar{y}^{(2)}\left(t_\varsigma\right) =&\Phi_{\sigma_{t_\varsigma+lh}}\check{y}^{(2)}\left(t_\varsigma+lh\right)+\left(I-\Phi_{\sigma_{t_\varsigma+lh}}\right)\bar{y}^{(2)}\left(t_{\varsigma-1}\right)\\ =&\Phi_{\sigma_{t_\varsigma+lh}}\left(\widetilde{P}_2\bar{y}^{(2)}(t_\varsigma+lh)+\mathcal{I}_2\bar{\mathcal{A}}\left(t_\varsigma\right)\right)\\ &+\left(I-\Phi_{\sigma_{t_\varsigma+lh}}\right)\bar{y}^{(2)}\left(t_{\varsigma-1}\right)\\ =&\Phi_{\sigma_{t_\varsigma+lh}}\widetilde{P}_2 y^{(2)}\left(t_\varsigma+l_h\right)-\Phi_{\sigma_{t_\varsigma+lh}}\widetilde{P}_2\mathcal{I}_2\bar{\varphi}\left(t_\varsigma\right)\\ &+\Phi_{\sigma_{t_\varsigma+lh}}\mathcal{I}_2\bar{\mathcal{A}}\left(t_\varsigma\right)+\left(I-\Phi_{\sigma_{t_\varsigma+lh}}\right)\bar{y}^{(2)}\left(t_{\varsigma-1}\right)\\ =&\acute{C}\left(t_\varsigma\right)\bar{x}\left(t_\varsigma\right)+\acute{D}\left(t_\varsigma\right)\bar{v}\left(t_\varsigma\right)+\acute{H}\left(t_\varsigma\right)\eta\left(t_\varsigma\right)\\ &+\left(I-\Phi_{\sigma_{t_\varsigma+lh}}\right)\bar{y}^{(2)}\left(t_{\varsigma-1}\right).\end{aligned} \tag{30}$$

Then, it follows from (29) and (30) that

$$\bar{y}\left(t_\varsigma\right)=\ell_1\bar{y}^{(1)}\left(t_\varsigma\right)+\ell_2\bar{y}^{(2)}\left(t_\varsigma\right), \tag{31}$$

which indicates that (28) is satisfied, thus concluding the proof of this lemma. ■

Remark 4: It is important to note that during network transmission, we consider the scenario where only the measurement output data from sensor nodes that have obtained transmission permission undergo probabilistic bit flips. As a result, the output data after network transmission is not only influenced by the FRP but is also directly related to the possible bit flips.

2.6. Bit-Flip and FlexRay-Protocol-Based Estimation Design

So far, we have introduced bit flips occurring during signal transmission and the operational principles of FRP. Next, we will investigate and analyze the final impact on the design of the state estimator, resulting from signals affected by probabilistic bit flips within a single communication cycle after being transmitted through the FlexRay network.

Before considering the design of the state estimator for the underlying systems in this section, we firstly derive an augmented system that integrates the system state $\bar{x}^{\mathrm{T}}\left(t_\varsigma\right)$ with the holding term $\bar{y}^{(2)}\left(t_{\varsigma-1}\right)$. The resulting formula is expressed as:

$$\begin{cases}\tilde{x}\left(t_{\varsigma+1}\right) =\check{A}\left(t_\varsigma\right)\tilde{x}\left(t_\varsigma\right)+\check{B}\left(t_\varsigma\right)\varpi\left(t_\varsigma\right)+\check{H}\eta\left(t_\varsigma\right)\\ \bar{y}\left(t_\varsigma\right) =\check{C}\left(t_\varsigma\right)\tilde{x}\left(t_\varsigma\right)+\check{\mathcal{D}}\left(t_\varsigma\right)\varpi\left(t_\varsigma\right)+H\eta\left(t_\varsigma\right)\end{cases} \tag{32}$$

where

$$\begin{aligned}&\tilde{x}\left(t_\varsigma\right)\triangleq\left[\bar{x}^{\mathrm{T}}\left(t_\varsigma\right)\quad\left(\bar{y}^{(2)}\left(t_{\varsigma-1}\right)\right)^{\mathrm{T}}\right]^{\mathrm{T}},\\ &\check{A}\left(t_\varsigma\right)\triangleq\begin{bmatrix}\bar{\mathcal{A}}\left(t_\varsigma\right) & 0\\ \acute{C}\left(t_\varsigma\right) & I-\Phi_{\sigma_{t_\varsigma+lh}}\end{bmatrix},\\ &\check{B}\left(t_\varsigma\right)\triangleq\begin{bmatrix}\bar{\mathcal{B}}\left(t_\varsigma\right) & 0\\ 0 & \acute{D}\left(t_\varsigma\right)\end{bmatrix},\\ &\check{C}\left(t_\varsigma\right)\triangleq\begin{bmatrix}\hat{C}\left(t_\varsigma\right) & \ell_2\left(I-\Phi_{\sigma_{t_\varsigma+lh}}\right)\end{bmatrix},\\ &\check{\mathcal{D}}\triangleq\left[\underbrace{0,\cdots,0}_{w},\ \check{D}\left(t_\varsigma\right)\right],\\ &\check{H}\left(t_\varsigma\right)\triangleq\left[0^{\mathrm{T}}\quad\check{H}^{\mathrm{T}}\left(t_\varsigma\right)\right]^{\mathrm{T}},\\ &\varpi\left(t_\varsigma\right)\triangleq\left[\bar{w}^{\mathrm{T}}\left(t_\varsigma\right)\quad\bar{v}^{\mathrm{T}}\left(t_\varsigma\right)\right]^{\mathrm{T}}.\end{aligned}$$

Based on (28) and (32), the following estimator for the time-varying state is developed:

$$\hat{x}\left(t_{\varsigma+1}\right)=\breve{A}(t_{\varsigma})\hat{x}\left(t_{\varsigma}\right)+L\left(t_{\varsigma}\right)\left(\bar{y}\left(t_{\varsigma}\right)-\breve{C}\left(t_{\varsigma}\right)\hat{x}\left(t_{\varsigma}\right)\right) \tag{33}$$

where $\hat{x}(t_{\varsigma})\in\mathbb{R}^{f_n+m-l}$ represents the state estimate for $\tilde{x}(t_{\varsigma})$, $L(t_{\varsigma})\in\mathbb{R}^{(f_n+m-l)\times m}$ denotes the time-varying parameter of the state estimator that needs to be determined.

The estimation error, denoted as $e\left(t_{\varsigma}\right)$, is defined as the difference between the augmented system vector $\tilde{x}\left(t_{\varsigma}\right)$ and the estimated state vector $\hat{x}\left(t_{\varsigma}\right)$. The derivation of the dynamics of this error can be obtained from equations (32) and (33) as follows:

$$e\left(t_{\varsigma+1}\right)=\tilde{A}\left(t_{\varsigma}\right)e\left(t_{\varsigma}\right)+\tilde{B}\left(t_{\varsigma}\right)\varpi\left(t_{\varsigma}\right)+\bar{H}\left(t_{\varsigma}\right)\eta\left(t_{\varsigma}\right) \tag{34}$$

where

$$\begin{aligned}\tilde{A}\left(t_{\varsigma}\right)&\triangleq\breve{A}\left(t_{\varsigma}\right)-L\left(t_{\varsigma}\right)\breve{C}\left(t_{\varsigma}\right),\\ \tilde{B}\left(t_{\varsigma}\right)&\triangleq\breve{B}\left(t_{\varsigma}\right)-L\left(t_{\varsigma}\right)\breve{\mathcal{D}}\left(t_{\varsigma}\right),\\ \bar{H}\left(t_{\varsigma}\right)&\triangleq\breve{H}\left(t_{\varsigma}\right)-L\left(t_{\varsigma}\right)H\left(t_{\varsigma}\right).\end{aligned}$$

Definition 1: [36,37] Assume that there exist positive scalars d_1, d_2, d_3, $0<\delta_x<\varepsilon$, and a positive definite matrix R. Consider the linear discrete time-varying system (34) subject to the disturbance vector $\varpi\left(t_{\varsigma}\right)$ and error vector $\eta\left(t_{\varsigma}\right)$ satisfying $\bar{w}^{\mathrm{T}}\left(t_{\varsigma}\right)\bar{w}\left(t_{\varsigma}\right)<d_1$ and $\bar{v}^{\mathrm{T}}\left(t_{\varsigma}\right)\bar{v}\left(t_{\varsigma}\right)<d_2$, respectively. The system (34) is deemed to be FTB relative to the parameters $(\delta_x,\varepsilon,R,d_1,d_2,d_3,N)$ if the constraint $\mathbb{E}\left\{e^{\mathrm{T}}\left(t_{\varsigma}\right)Re\left(t_{\varsigma}\right)\right\}\leqslant\varepsilon^2$ holds for all $t_{\varsigma}\in\{1,\cdots,N\}$ under the condition $e^{\mathrm{T}}(0)Re(0)\leqslant\delta_x^2$.

Now, we can summarize the main purpose of this article as follows: the aim of this paper is to develop a state estimator for the error system (34) utilizing bit-flipping and the FRP, ensuring that the dynamics of system (34) remain bounded over a finite time horizon under the combined influence of disturbance noise $\varpi\left(t_{\varsigma}\right)$ and the error $\eta\left(t_{\varsigma}\right)$ introduced by quantization and bit-flipping processes. In the subsequent chapters, we will present sufficient conditions to guarantee that the estimation error is bounded within a finite time horizon. The desired estimator gains will be obtained by solving the corresponding recursive LMIs presented later.

3. Main Results

In this section, a sufficient condition for the finite-time boundedness of the error system (34) is presented. Based on this, the required state estimator parameters will be obtained by solving a recursive matrix inequality problem.

Theorem 1: Let a scalar $\gamma>0$ be given and assume that there exist three symmetric positive definite matrices $P_1\left(t_{\varsigma}\right)$, $P_2\left(t_{\varsigma}\right)$ and $P_3\left(t_{\varsigma}\right)$ with appropriate dimensions such that the following conditions hold. Then, the system (34) is FTB with respect to the parameters $(\delta_x,\varepsilon,R,d_1,d_2,d_3,N)$ if the following condition holds:

$$\begin{bmatrix}-\gamma P_1\left(t_{\varsigma}\right) & 0 & 0 & \tilde{A}^{\mathrm{T}}\left(t_{\varsigma}\right)\\ * & -\gamma P_2\left(t_{\varsigma}\right) & 0 & \tilde{B}^{\mathrm{T}}\left(t_{\varsigma}\right)\\ * & * & -\gamma P_3\left(t_{\varsigma}\right) & \bar{H}^{\mathrm{T}}\left(t_{\varsigma}\right)\\ * & * & * & -P_1^{-1}\left(t_{\varsigma+1}\right)\end{bmatrix}<0 \tag{35}$$

$$\lambda_1\delta_x^2+\lambda_2(d_1+d_2)\frac{1-\frac{1}{\gamma^N}}{1-\frac{1}{\gamma}}+\lambda_3 d_3\frac{1-\frac{1}{\gamma^N}}{1-\frac{1}{\gamma}}<\frac{\varepsilon^2\lambda_4}{\gamma^N} \tag{36}$$

where $\bar{P}_1\left(t_{\varsigma}\right)\triangleq R^{-\frac{1}{2}}P_1\left(t_{\varsigma}\right)R^{-\frac{1}{2}}$, $\gamma>0$ denotes the stable index and

$$\begin{aligned}&\lambda_1\triangleq\max_{t_{\varsigma}\in N}\left\{\lambda_{\max}(\bar{P}_1(t_{\varsigma}))\right\},\ \tilde{A}\left(t_{\varsigma}\right)\triangleq\breve{A}\left(t_{\varsigma}\right)-L\left(t_{\varsigma}\right)\breve{C}\left(t_{\varsigma}\right),\\ &\lambda_3\triangleq\max_{t_{\varsigma}\in N}\left\{\lambda_{\max}\left(P_3\left(t_{\varsigma}\right)\right)\right\},\ \tilde{B}\left(t_{\varsigma}\right)\triangleq\breve{B}(t_{\varsigma})-L(t_{\varsigma})\breve{\mathcal{D}}\left(t_{\varsigma}\right),\\ &\lambda_2\triangleq\max_{t_1\in N}\left\{\lambda_{\max}\left(P_2\left(t_{\varsigma}\right)\right)\right\},\ \lambda_4\triangleq\min_{t_{\varsigma}\in N}\left\{\lambda_{\min}\left(\bar{P}_1\left(t_{\varsigma}\right)\right)\right\},\\ &\bar{H}\left(t_{\varsigma}\right)\triangleq\breve{H}\left(t_{\varsigma}\right)-L\left(t_{\varsigma}\right)H\left(t_{\varsigma}\right).\end{aligned}$$

Proof: To maintain generality, we suppose that $\bar{w}^{\mathrm{T}}\left(t_{\varsigma}\right)\bar{w}\left(t_{\varsigma}\right)<d_1$, $\bar{v}^{\mathrm{T}}\left(t_{\varsigma}\right)\bar{v}\left(t_{\varsigma}\right)<d_2$ and $e^{\mathrm{T}}(0)Re(0)\leqslant\delta_x^2$. According to the definition of $\varpi\left(t_{\varsigma}\right)$, it is easy to have $\varpi^{\mathrm{T}}\left(t_{\varsigma}\right)\varpi\left(t_{\varsigma}\right)<d_1+d_2$. Let the Lyapunov candidate be $V\left(t_{\varsigma}\right)=e^{T}\left(t_{\varsigma}\right)P_1\left(t_{\varsigma}\right)e\left(t_{\varsigma}\right)$. Then, we have

$$\begin{aligned} V\left(t_{\varsigma+1}\right) &= e^{\mathrm{T}}\left(t_{\varsigma+1}\right) P_1\left(t_{\varsigma+1}\right) e\left(t_{\varsigma+1}\right) \\ &= \begin{bmatrix} e\left(t_\varsigma\right) \\ \varpi\left(t_\varsigma\right) \\ \eta\left(t_\varsigma\right) \end{bmatrix}^{\mathrm{T}} \xi^{\mathrm{T}}\left(t_\varsigma\right) P_1\left(t_{\varsigma+1}\right) \xi\left(t_\varsigma\right) \begin{bmatrix} e\left(t_\varsigma\right) \\ \varpi\left(t_\varsigma\right) \\ \eta\left(t_\varsigma\right) \end{bmatrix} \end{aligned} \tag{37}$$

where $\xi\left(t_\varsigma\right) = \begin{bmatrix} \widetilde{A}\left(t_\varsigma\right) & \widetilde{B}\left(t_\varsigma\right) & \bar{H}\left(t_\varsigma\right) \end{bmatrix}$.

Assuming that the condition

$$\begin{aligned} V\left(t_{\varsigma+1}\right) \leqslant & \gamma V\left(t_\varsigma\right) + \gamma \varpi^{\mathrm{T}}\left(t_\varsigma\right) P_2\left(t_\varsigma\right) \varpi^{\mathrm{T}}\left(t_\varsigma\right) \\ & + \gamma \eta^{\mathrm{T}}\left(t_\varsigma\right) P_3\left(t_\varsigma\right) \eta\left(t_\varsigma\right) \end{aligned} \tag{38}$$

holds. In the following text, we will first prove that the system described by formula (34) exhibits finite-time boundedness with respect to the parameters $(\delta_x, \varepsilon, R, d_1, d_2, d_3, N)$ if the inequality (38) and the condition (36) hold. And then, to finalize the proof, we will proof that the conditions (38) is equivalent to (35).

Letting $\bar{P}_1\left(t_\varsigma\right) = R^{-\frac{1}{2}} P_1\left(t_\varsigma\right) R^{-\frac{1}{2}}$, $\gamma > 0$ and

$$\lambda_1 \triangleq \max_{t_\varsigma \in N}\left\{\lambda_{\max}\left(\bar{P}_1\left(t_\varsigma\right)\right)\right\},\ \lambda_2 \triangleq \max_{t_1 \in N}\left\{\lambda_{\max}\left(P_2\left(t_\varsigma\right)\right)\right\}, \lambda_3 \triangleq \max_{t_\varsigma \in N}\left\{\lambda_{\max}\left(P_3\left(t_\varsigma\right)\right)\right\},\ \lambda_4 \triangleq \min_{t_\varsigma \in N}\left\{\lambda_{\min}\left(\bar{P}_1\left(t_\varsigma\right)\right)\right\}.$$

Besides, consider

$$\begin{aligned} & \mathbb{E}\left\{\eta^{\mathrm{T}}\left(t_\varsigma\right) \eta\left(t_\varsigma\right)\right\} \\ \leqslant & \sum_{i=1}^{m} \frac{\sigma_i^2}{\widetilde{\Delta}_i^2} + \sum_{i=1}^{m} \frac{4}{3} \bar{\rho}_i\left(1-\bar{\rho}_i\right) \frac{\sigma_i^2\left(2^{2\Lambda i}-1\right)}{2^{2\Lambda_i}} \end{aligned}$$

and to simplify the expression further, let $d_3 \triangleq \sum_{i=1}^{m} \frac{\sigma_i^2}{\widetilde{\Delta}_i^2} + \sum_{i=1}^{m} \frac{4}{3} \bar{\rho}_1\left(1-\bar{\rho}_i\right) \frac{\sigma_i^2\left(2^{2\Lambda i}-1\right)}{2^{2\Lambda_i}}$, and then, by iterating equation (38) and taking the expectation on both sides, we can obtain the following expression:

$$\begin{aligned} & \mathbb{E}\left\{V\left(t_\varsigma\right)\right\} \leqslant \gamma^\varsigma \mathbb{E}\{V(t_0)\} \\ & + \mathbb{E}\left\{\sum_{i=1}^{\varsigma} \gamma^i \varpi^{\mathrm{T}}\left(t_\varsigma\right) P_2\left(t_{\varsigma-i}\right) \varpi\left(t_\varsigma\right)\right\} \\ & + \mathbb{E}\left\{\sum_{i=1}^{\varsigma} \gamma^i \eta^{\mathrm{T}}\left(t_{\varsigma-i}\right) P_3\left(t_{\varsigma-i}\right) \eta\left(t_{\varsigma-i}\right)\right\} \\ \leqslant & \gamma^\varsigma e^{\mathrm{T}}(t_0) P_1(t_0) e(t_0) \\ & + \lambda_2(d_1+d_2)\frac{\gamma^{\varsigma+1}-\gamma}{\gamma-1} + \lambda_3 d_3 \frac{\gamma^{\varsigma+1}-\gamma}{\gamma-1} \\ \leqslant & \gamma^\varsigma \lambda_1 \delta_x^2 + \lambda_2(d_1+d_2)\frac{\gamma^{\varsigma+1}-\gamma}{\gamma-1} + \lambda_3 d_3 \frac{\gamma^{\varsigma+1}-\gamma}{\gamma-1} \\ \leqslant & \gamma^N \left[\lambda_1 \delta_x^2 + \lambda_2(d_1+d_2)\frac{1-\frac{1}{\gamma^N}}{1-\frac{1}{\gamma}} + \lambda_3 d_3 \frac{1-\frac{1}{\gamma^N}}{1-\frac{1}{\gamma}}\right]. \end{aligned} \tag{39}$$

Noticing that

$$\begin{aligned} \mathbb{E}\left\{V\left(t_\varsigma\right)\right\} &= \mathbb{E}\left\{e^{\mathrm{T}}\left(t_\varsigma\right) P_1\left(t_\varsigma\right) e\left(t_\varsigma\right)\right\} \\ &\geqslant \lambda_4 \mathbb{E}\left\{e^{\mathrm{T}}\left(t_\varsigma\right) R e^{\mathrm{T}}\left(t_\varsigma\right)\right\} \end{aligned} \tag{40}$$

and by combining equations (39) and (40), we obtain

$$\begin{aligned} & \mathbb{E}\left\{e^{\mathrm{T}}\left(t_\varsigma\right) R e\left(t_\varsigma\right)\right\} \\ < & \frac{\gamma^N}{\lambda_4}\left[\lambda_1 \delta_x^2 + \lambda_2(d_1+d_2)\frac{1-\frac{1}{\gamma^N}}{1-\frac{1}{\gamma}} + \lambda_3 d_3 \frac{1-\frac{1}{\gamma^N}}{1-\frac{1}{\gamma}}\right]. \end{aligned} \tag{41}$$

From (41), we can know that (36) implies $\forall \varsigma \in \{1, \cdots, N\}$, $\mathbb{E}\left\{e^{\mathrm{T}}\left(t_\varsigma\right) R e\left(t_\varsigma\right)\right\} \leqslant \varepsilon^2$. Thus, the system (34) exhibits finite-time boundedness with respect to the parameters $(\delta_x, \varepsilon, R, d_1, d_2, d_3, N)$.

Next, let's prove that condition (38) is equivalent to (35).

Formula (38) can be rewritten as follows:

$$\begin{aligned}&\xi^{\mathrm{T}}\left(t_{\varsigma}\right)P_1\left(t_{\varsigma+1}\right)\xi\left(t_{\varsigma}\right)\\&+\begin{bmatrix}-\gamma P_1\left(t_{\varsigma}\right) & 0 & 0\\ 0 & -\gamma P_2\left(t_{\varsigma}\right) & 0\\ 0 & 0 & -\gamma P_3\left(t_{\varsigma}\right)\end{bmatrix}<0.\end{aligned}\tag{42}$$

Employing Schur complements, (42) can be considered equivalent to

$$\begin{bmatrix}-\gamma P_1\left(t_{\varsigma}\right) & 0 & 0 & \tilde{A}^{\mathrm{T}}\left(t_{\varsigma}\right)\\ * & -\gamma P_2\left(t_{\varsigma}\right) & 0 & \tilde{B}^{\mathrm{T}}\left(t_{\varsigma}\right)\\ * & * & -\gamma P_3\left(t_{\varsigma}\right) & \bar{H}^{\mathrm{T}}\left(t_{\varsigma}\right)\\ * & * & * & -P_1^{-1}\left(t_{\varsigma+1}\right)\end{bmatrix}<0.\tag{43}$$

From (43), we can obtain that (38) is equivalent to (35). Then, the proof is complete.

Remark 5: In the estimation error system, the system noise and measurement noise are both energy-bounded, and the error terms resulting from quantization errors and bit-flip processes are also bounded. Consequently, within given initial conditions and a finite time horizon, the system is upper-bounded, meaning that the error between the estimates provided by the estimator and the actual values remains within a certain range for a finite duration.

Remark 6: The existing literature on finite-time boundedness primarily focuses on the study of system control performance. In these works, finite-time boundedness typically describes the boundedness of the system's state over a finite time interval, given initial conditions and the influence of external disturbances, which can be regarded as an extension of finite-time stability. This paper extends this concept to the problem of state estimation, investigating the boundedness of the estimation error over a finite-time horizon.

Next, we will focus on the design of the gain matrix $L\left(t_{\varsigma}\right)$ for the state estimator under the effects of FRP scheduling and bit flips. More specifically, we would like to complete the design of the estimator through calculating the estimator parameter $L\left(t_{\varsigma}\right)$ by solving certain recursive matrix inequalities.

Corollary 1: Given a scalar $\gamma>0$, $0<\delta_x<\varepsilon$, the positive integer N and a positive definite matrix R. Assume there exist four symmetric positive definite matrices $Q\left(t_{\varsigma}\right)$, $P_1\left(t_{\varsigma}\right)$, $P_2\left(t_{\varsigma}\right)$ and $P_3\left(t_{\varsigma}\right)$ with appropriate dimensions such that the following conditions hold, then, the state estimator gain $L(t_{\varsigma})$ of system (33) can be obtained by solving the following matrix inequalities:

$$\begin{bmatrix}-\gamma P_1\left(t_{\varsigma}\right) & 0 & 0 & \tilde{A}^{\mathrm{T}}\left(t_{\varsigma}\right)\\ * & -\gamma P_2\left(t_{\varsigma}\right) & 0 & \tilde{B}^{\mathrm{T}}\left(t_{\varsigma}\right)\\ * & * & -\gamma P_3\left(t_{\varsigma}\right) & \bar{H}^{\mathrm{T}}\left(t_{\varsigma}\right)\\ * & * & * & -Q\left(t_{\varsigma+1}\right)\end{bmatrix}<0\tag{44}$$

$$P_1\left(t_{\varsigma+1}\right)+Q\left(t_{\varsigma+1}\right)\leqslant 2I\tag{45}$$

$$\lambda_1\delta_x^2+\lambda_2(d_1+d_2)\frac{1-\frac{1}{\gamma^N}}{1-\frac{1}{\gamma}}+\lambda_3 d_3\frac{1-\frac{1}{\gamma^N}}{1-\frac{1}{\gamma}}<\frac{\varepsilon^2\lambda_4}{\gamma^N}\tag{46}$$

Proof: Now, we will prove that if formulas (44) and (45) hold, then (43) holds as well, i.e., solving for the estimator parameters is equivalent to solving the recursive matrix inequalities (44) and (45).

It is not difficult to see from (42) and (45) that:

$$\begin{aligned}&\xi^{\mathrm{T}}\left(t_{\varsigma}\right)P_1\left(t_{\varsigma+1}\right)\xi\left(t_{\varsigma}\right)\\&+\begin{bmatrix}-\gamma P_1\left(t_{\varsigma}\right) & 0 & 0\\ 0 & -\gamma P_2\left(t_{\varsigma}\right) & 0\\ 0 & 0 & -\gamma P_3\left(t_{\varsigma}\right)\end{bmatrix}\\&\leqslant\xi^{\mathrm{T}}\left(t_{\varsigma}\right)Q^{-1}\left(t_{\varsigma+1}\right)\xi\left(t_{\varsigma}\right)\\&+\begin{bmatrix}-\gamma P_1\left(t_{\varsigma}\right) & 0 & 0\\ 0 & -\gamma P_2\left(t_{\varsigma}\right) & 0\\ 0 & 0 & -\gamma P_3\left(t_{\varsigma}\right)\end{bmatrix}.\end{aligned}\tag{47}$$

Then, by applying the Schur complement, the following can be obtained

$$\begin{aligned}
&\xi^{\mathrm{T}}\left(t_{\varsigma}\right) Q^{-1}\left(t_{\varsigma+1}\right) \xi\left(t_{\varsigma}\right) \\
&+\begin{bmatrix} -\gamma P_1\left(t_{\varsigma}\right) & 0 & 0 \\ 0 & -\gamma P_2\left(t_{\varsigma}\right) & 0 \\ 0 & 0 & -\gamma P_3\left(t_{\varsigma}\right) \end{bmatrix} \\
&=\begin{bmatrix} -\gamma P_1\left(t_{\varsigma}\right) & 0 & 0 & \tilde{A}^{\mathrm{T}}\left(t_{\varsigma}\right) \\ * & -\gamma P_2\left(t_{\varsigma}\right) & 0 & \tilde{B}^{\mathrm{T}}\left(t_{\varsigma}\right) \\ * & * & -\gamma P_3\left(t_{\varsigma}\right) & \tilde{H}^{\mathrm{T}}\left(t_{\varsigma}\right) \\ * & * & * & -Q\left(t_{\varsigma+1}\right) \end{bmatrix}.
\end{aligned} \tag{48}$$

Finally, from (44), it is clear that the proof is complete, and the proof concludes.

Remark 7: Up to this point, we have addressed the state estimation problem for time-varying systems under the effects of FRP scheduling and bit-flipping phenomena. First, we established an augmented model for the system after network transmission and constructed a state estimator with a simple structure. Then, in Theorem 3.1, we derived the sufficient conditions for the boundedness of the error system within a finite time horizon, and in Corollary 1, we derived the required state estimator gains.

4. Illustrative Examples

In this section, the effectiveness of the proposed state estimator design scheme based on the FRP and probabilistic bit-flipping is validated through two simulation examples.

Example 1: We consider the parameters of the time-varying system (1) as follows:

$$A\left(T_{\varsigma}\right)=\begin{bmatrix} a_1\left(T_{\varsigma}\right) & 0.25 & 0 & 0 & 0 \\ -0.1 & a_2\left(T_{\varsigma}\right) & 0 & 0 & 0 \\ 0.5 & 0 & a_3\left(T_{\varsigma}\right) & 0 & 0 \\ 0.6 & 0 & a_4\left(T_{\varsigma}\right) & -0.2 & 0 \\ -0.1 & 0.3 & 0 & 0 & 0.1 \end{bmatrix},$$

$$B\left(T_{\varsigma}\right)=\begin{bmatrix} -0.4+0.2\sin\left(2T_{\varsigma}\right) \\ 0.2 \\ -0.1 \\ -0.5 \\ 0 \end{bmatrix},$$

$$C\left(T_{\varsigma}\right)=\begin{bmatrix} c_1\left(T_{\varsigma}\right) & 0.2 & 0 & 0 & 0 \\ 0 & c_2\left(T_{\varsigma}\right) & -0.2 & 0 & 0 \\ 0 & 0 & 2 & 0 & 0 \\ 0 & 0 & 0 & 1 & 0 \end{bmatrix},$$

$$D(T_K)=\begin{bmatrix} 0.12 \\ -0.1+0.2\cos\left(T_{\varsigma}\right) \\ 0.3 \\ -0.2 \end{bmatrix},$$

$$w\left(T_{\varsigma}\right)=0.2\sin\left(-T_{\varsigma}\right),\ v\left(T_{\varsigma}\right)=0.1\cos\left(-2T_{\varsigma}\right)$$

where

$$\begin{aligned}
a_1\left(T_{\varsigma}\right)&=1.12+0.2\sin\left(2T_{\varsigma}\right), \\
a_2\left(T_{\varsigma}\right)&=0.16-0.2\cos\left(3T_{\varsigma}\right), \\
a_3\left(T_{\varsigma}\right)&=-0.6-0.1\sin\left(T_{\varsigma}\right), \\
a_4\left(T_{\varsigma}\right)&=0.1+0.4\sin\left(T_{\varsigma}\right), \\
c_1\left(T_{\varsigma}\right)&=0.5+0.3\cos\left(-2T_{\varsigma}\right), \\
c_2\left(T_{\varsigma}\right)&=0.6-0.1\cos\left(3T_{\varsigma}\right).
\end{aligned}$$

The initial value of $P_1\left(t_{\varsigma}\right)$ is set as $P_1(0)=I$, and the initial state and its corresponding estimated state are given as follows:

$$\begin{aligned}
&x_1(0)=-0.18,\ x_2(0)=0.15,\ x_3(0)=0.18,\ x_4(0)=-0.1, \\
&x_5(0)=0.5,\ \hat{x}_1(0)=\hat{x}_2(0)=\hat{x}_3(0)=\hat{x}_4(0)=\hat{x}_5(0)=0.
\end{aligned}$$

The flip probabilities of each bit for the output value of sensor nodes are given as

$$\bar{\rho}_1 = 0.01, \quad \bar{\rho}_2 = 0.14, \quad \bar{\rho}_3 = 0.03, \quad \bar{\rho}_4 = 0.12$$

and $Q_3(T_\varsigma) = 2, Q_4(T_\varsigma) = 1.5$, $d_1 = 0.05$, $d_2 = 0.02$, $\Lambda i = 7$, $R = 0.1I$, $\delta_x = 0.4$. Set the step size $N = 90$, $h = 1$, $l = 2$, and the stable index $\gamma = 0.9$.

According to our proposed estimator design method, we can calculate the estimator parameter recursively. Based on the achieved time-varying estimator parameter, the system state and its estimation are illustrated in Figures 3–7. Figure 8 depicts the estimation error curves for each state, verifying that the estimation errors are indeed FTB. The simulation results shown by these figures confirm that the resultant estimation performance is satisfactory.

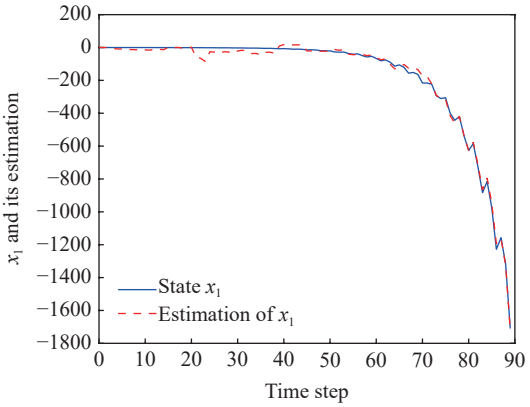

Figure 3. State x_1 and its estimation.

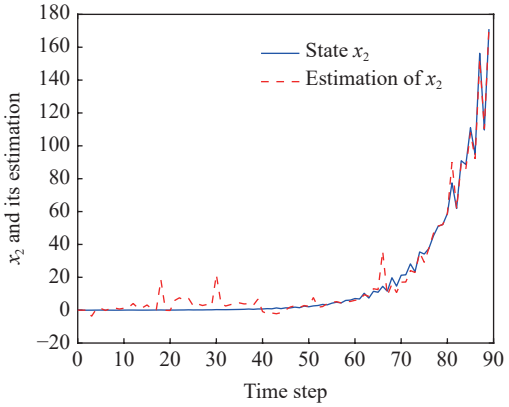

Figure 4. State x_2 and its estimation.

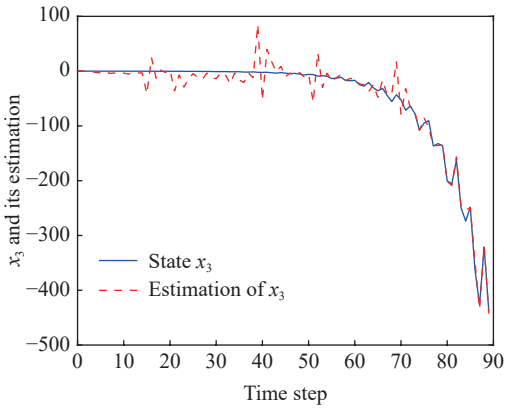

Figure 5. State x_3 and its estimation.

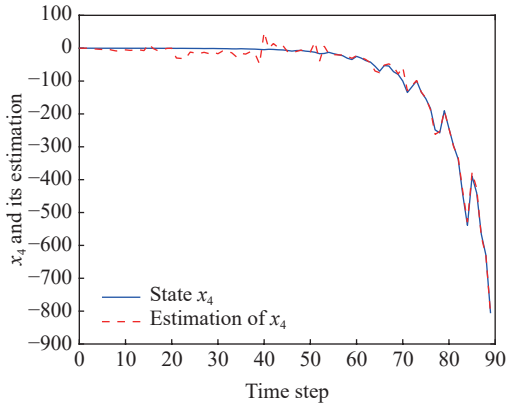

Figure 6. State x_4 and its estimation.

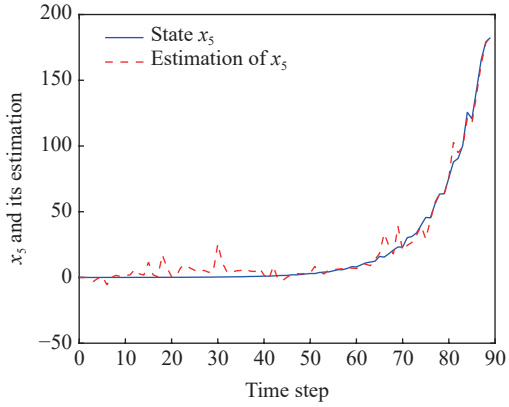

Figure 7. State x_5 and its estimation.

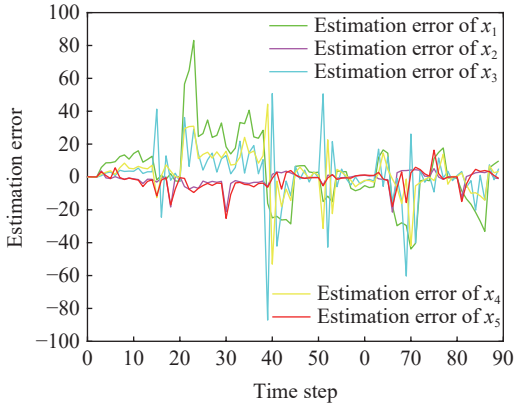

Figure 8. Estimation errors e_1, e_2, e_3, e_4, e_5 under FRP.

Under the condition that both the system and simulation parameters remain unchanged, the protocol is switched to RRP, and the same estimation algorithm is applied. The estimation errors of the system states are shown in Figure 9, while Table 2 presents the mean squared estimation errors for different states under both the FRP and RRP protocols. It can be observed that the FRP exhibits its inherent advantages when applied with the algorithm presented in this paper.

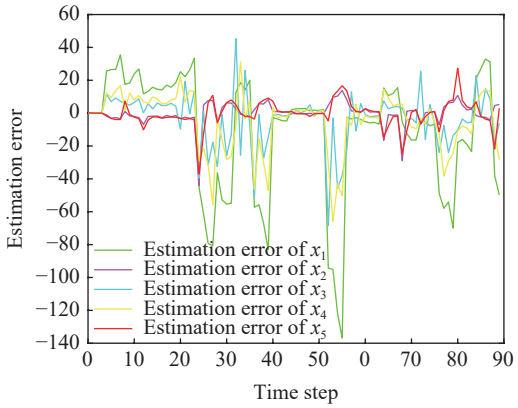

Figure 9. Estimation errors e_1, e_2, e_3, e_4, e_5 under RRP.

Table 2 The Mean Squared Error of System States Under Different Protocols

System States	Protocol	Mean Squared Error
x_1	FlexRay	473.9069
	Round-Robin	1480.7921
x_2	FlexRay	22.5701
	Round-Robin	50.7732
x_3	FlexRay	358.1316
	Round-Robin	290.1564
x_4	FlexRay	187.3245
	Round-Robin	351.4839
x_5	FlexRay	35.5596
	Round-Robin	66.0894

Example 2: Let us now apply the proposed algorithm to a 6-node system to demonstrate the scalability of the method. The system (1) parameters considered are as follows:

$$A\left(T_\varsigma\right)=\begin{bmatrix} a_1\left(T_\varsigma\right) & 0.25 & 0.1 & 0 & 0 & 0 \\ -0.1 & a_2\left(T_\varsigma\right) & 0 & 0 & 0 & 0.1 \\ 0.5 & 0 & a_3\left(T_\varsigma\right) & 0 & 0 & 0 \\ 0.6 & 0 & a_4\left(T_\varsigma\right) & -0.2 & 0 & 0 \\ -0.1 & 0.3 & 0 & 0 & 0.1 & 0 \\ 0.1 & -0.2 & 0 & 0 & 0.1 & 0.3 \end{bmatrix},$$

$$B\left(T_\varsigma\right)=\begin{bmatrix} -0.4+0.2\sin\left(2T_\varsigma\right) \\ 0.2 \\ -0.1 \\ -0.5 \\ 0 \\ 0 \end{bmatrix},$$

$$C\left(T_\varsigma\right)=\begin{bmatrix} c_1\left(T_\varsigma\right) & 0.2 & 0 & 0 & 0 & 0 \\ 0 & c_2\left(T_\varsigma\right) & -0.2 & 0 & 0 & 0 \\ 0 & 0 & 2 & 0 & 0 & 0 \\ 0 & 0 & 0 & 1 & 0 & 0 \\ 1 & 0 & 0 & 0 & 0 & 0 \\ 0 & 0 & 0 & 0 & 0 & 1 \end{bmatrix},$$

$$D\left(T_K\right)=\begin{bmatrix} 0.12 \\ -0.1+0.2\cos\left(T_\varsigma\right) \\ 0.3 \\ -0.2 \\ 0.1 \end{bmatrix},$$

$$w\left(T_\varsigma\right)=0.2\sin\left(-T_\varsigma\right),\ v\left(T_\varsigma\right)=0.1\cos\left(-2T_\varsigma\right)$$

where

$$
\begin{aligned}
a_1\left(T_\varsigma\right) &= 1.12+0.2\sin\left(2T_\varsigma\right),\\
a_2\left(T_\varsigma\right) &= 0.16-0.2\cos\left(3T_\varsigma\right),\\
a_3\left(T_\varsigma\right) &= -0.6-0.1\sin\left(T_\varsigma\right),\\
a_4\left(T_\varsigma\right) &= 0.1+0.4\sin\left(T_\varsigma\right),\\
c_1\left(T_\varsigma\right) &= 0.5+0.3\cos\left(-2T_\varsigma\right),\\
c_2\left(T_\varsigma\right) &= 0.6-0.1\cos\left(3T_\varsigma\right).
\end{aligned}
$$

The initial state and its corresponding estimated state are given as follows:

$$x_0 = [-0.18, 0.15, 0.18, -0.1, 0.5, 0.1]^T,\ \hat{x}_0 = [0,0,0,0,0,0]^T$$

The flip probabilities of each bit for the output value of sensor nodes are given as

$$
\begin{aligned}
&\bar{\rho}_1 = 0.01, \quad \bar{\rho}_2 = 0.14, \quad \bar{\rho}_3 = 0.03,\\
&\bar{\rho}_4 = 0.12, \quad \bar{\rho}_5 = 0.1, \quad \bar{\rho}_6 = 0.05.
\end{aligned}
$$

And $Q_4\left(T_\varsigma\right) = 2, Q_5\left(T_\varsigma\right) = 1.5$, $h = 1$, $l = 4$. The other parameters can be found in example 1.

According to our proposed estimator design method, the system state and its estimation are illustrated in Figures 10–15. Figure 16 depicts the estimation error curves for each state, verifying that the estimation errors are indeed FTB. The simulation results further demonstrate the effectiveness and scalability of our estimation algorithm.

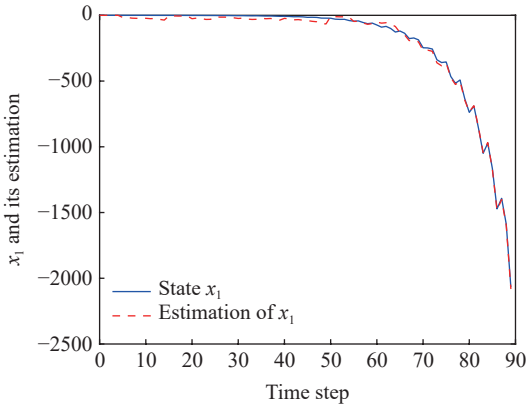

Figure 10. State x_1 and its estimation.

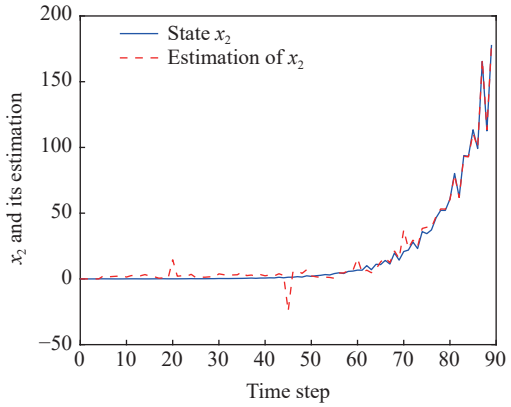

Figure 11. State x_2 and its estimation.

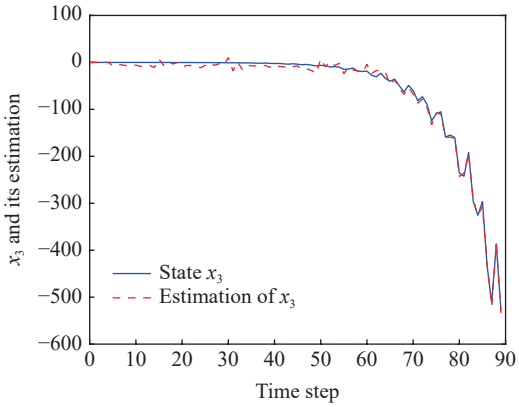

Figure 12. State x_3 and its estimation.

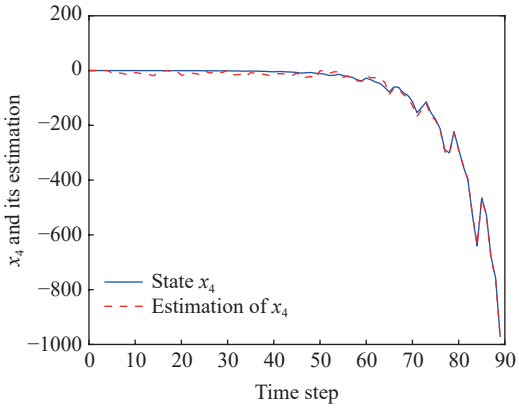

Figure 13. State x_4 and its estimation.

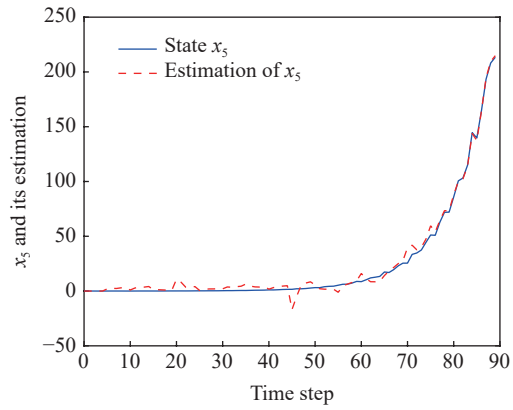

Figure 14. State x_5 and its estimation.

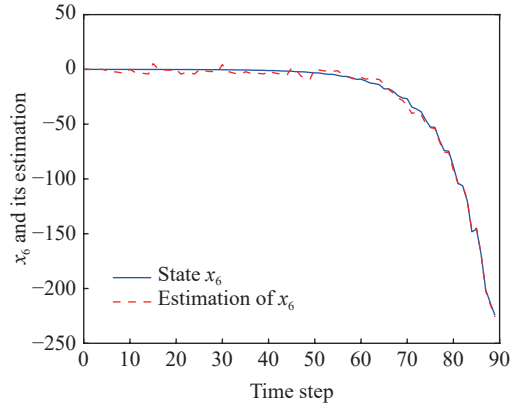

Figure 15. State x_6 and its estimation.

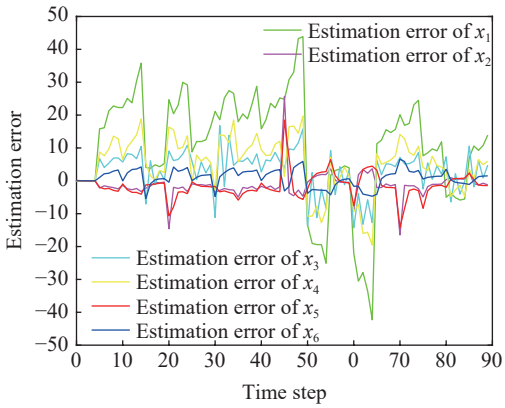

Figure 16. Estimation errors e_1, e_2, e_3, e_4, e_5, e_6.

5. Conclusion

In this paper, the problem of FTB state estimation for linear discrete time-varying systems with energy-bounded noise has been investigated under the FRP and probabilistic bit flips. The measurement outputs from sensors are transmitted to a state estimator through a communication network, adhering to the scheduling principles of the FRP and effects induced by an encoding-decoding mechanism. During the signal transmissions, measurement data are subject to the so-called probabilistic bit flips. Considering the combining effects induced by such a signal transmission process, a state estimator has been constructed to achieve the required finite-time boundedness. Then, sufficient conditions for ensuring such a requirement have been presented along with their proof processes. Finally, the effectiveness of the estimator design scheme has been validated through two simulation examples. Future research could explore the FTB state estimation for more complex systems (e.g., complex networks and multi-rate systems).

Author Contributions: **Lei Zou**; Investigation, **Hongli Ge** and **Lei Zou**; Methodology, **Hongli Ge**, **Lei Zou**, and **Hongwei Chen**; Supervision, **Lei Zou** and **Hongwei Chen**; Validation, **Hongli Ge**, **Lei Zou**, and **Jiyue Guo**; Writing-original draft, **Hongli Ge**; Writing-review and editing, **Hongli Ge**, **Lei Zou**, **Hongwei Chen**, and **Jiyue Guo**. All authors have read and agreed to the published version of the manuscript.

Funding: This work was supported in part by the National Natural Science Foundation of China under Grant 62273087, and the Natural Science Foundation of Shanghai under Grant 24ZR1400100.

Data Availability Statement: Not applicable.

Conflicts of Interest: The authors declare no conflict of interest.

Acknowledgments: The authors gratefully acknowledge the constructive comments and helpful suggestions from colleagues and reviewers, which have significantly contributed to the improvement of this manuscript.

References

1. Ciuonzo, D.; Aubry, A.; Carotenuto, V.. Rician MIMO channel-and jamming-aware decision fusion. IEEE Trans. Signal Process., **2017**, *65*: 3866−3880. doi: 10.1109/TSP.2017.2686375
2. G e, X.H.; Han, Q.L.; Zhang, X.M.;, *et al*. Distributed event-triggered estimation over sensor networks: A survey. IEEE Trans. Cybern., **2020**, *50*: 1306−1320. doi: 10.1109/TCYB.2019.2917179
3. H ou, N.; Dong, H.L.; Wang, Z.D.;, *et al*. A partial-node-based approach to state estimation for complex networks with sensor saturations under random access protocol. IEEE Trans. Neural Netw. Learn. Syst., **2021**, *32*: 5167−5178. doi: 10.1109/TNNLS.2020.3027252
4. L iu, S.; Wang, Z.D.; Wang, L.C.;, *et al*. Recursive set-membership state estimation over a FlexRay network. IEEE Trans. Syst., Man, Cybern.: Syst., **2022**, *52*: 3591−3601. doi: 10.1109/TSMC.2021.3071390
5. G uo, Y.R.; Wang, Z.D.; Li, J.Y.;, *et al*. State estimation for Markovian jump neural networks under probabilistic bit flips: Allocating constrained bit rates. IEEE Trans. Neural Netw. Learn. Syst., **2025**, *36*: 8802−8813. doi: 10.1109/tnnls.2024.3411484
6. Z ou, L.; Wang, Z.D.; Gao, H.J.;, *et al*. State estimation for discrete-time dynamical networks with time-varying delays and stochastic disturbances under the Round-Robin protocol. IEEE Trans. Neural Netw. Learn. Syst., **2017**, *28*: 1139−1151. doi: 10.1109/TNNLS.2016.2524621
7. Huong, D.C. Event-triggered finite-time guaranteed cost control of uncertain active suspension vehicle system. *J. Control Decis.* **2024**, in press. doi: 10.1080/23307706.2024.2423186

8. Cong Huong, D.. Design of event-triggered finite-time dissipative control for fractional-order time-delay interconnected systems. Circuits, Syst., Signal Process., **2025**, *44*: 3068−3087. doi: 10.1007/s00034-024-02992-9
9. L i, J.; Mu, X.W.; Li, K.. Event-triggered finite-time bounded and finite-time stability for Networked Control Systems under DoS attacks. Int. J. Syst. Sci., **2020**, *51*: 2820−2836. doi: 10.1080/00207721.2020.1802625
10. Sh en, Y.X.; Wang, Z.D.; Shen, B.;, *et al*. Recursive state estimation for networked multirate multisensor systems with distributed time-delays under Round-Robin protocol. IEEE Trans. Cybern., **2022**, *52*: 4136−4146. doi: 10.1109/TCYB.2020.3021350
11. Z ou, L.; Wang, Z.D.; Han, Q.L.;, *et al*. Ultimate boundedness control for networked systems with try-once-discard protocol and uniform quantization effects. IEEE Trans. Automat. Control, **2017**, *62*: 6582−6588. doi: 10.1109/TAC.2017.2713353
12. L iu, S.; Wang, Z.D.; Wang, L.C.;, *et al*. Finite-horizon H_∞ filtering via a high-rate network with the FlexRay protocol. IEEE Trans. Automat. Control, **2023**, *68*: 3596−3603. doi: 10.1109/TAC.2022.3190791
13. Wa ng, Y.Z.; Wang, Z.D.; Zou, L.;, *et al*. Ultimately bounded PID control for T–S fuzzy systems under FlexRay communication protocol. IEEE Trans. Fuzzy Syst., **2023**, *31*: 4308−4320. doi: 10.1109/TFUZZ.2023.3282044
14. Zhang, P.; Zhu, C.Q.; Wang, Z.W.;, *et al*. Recursive set-membership filtering for two-dimensional shift-varying systems with FlexRay protocol and hybrid cyber attacks. Asian J. Control, **2025**, *27*: 797−816. doi: 10.1002/asjc.3478
15. Lescanne, R.; Villiers, M.; Peronnin, T.;, *et al*. Exponential suppression of bit-flips in a qubit encoded in an oscillator. Nat. Phys., **2020**, *16*: 509−513. doi: 10.1038/s41567-020-0824-x
16. L iu, Q.Y.; Wang, Z.D.; Dong, H.L.;, *et al*. Remote estimation for energy harvesting systems under multiplicative noises: A binary encoding scheme with probabilistic bit flips. IEEE Trans. Automat. Control, **2023**, *68*: 343−354. doi: 10.1109/TAC.2022.3170540
17. Rakin, A.S.; He, Z.Z.; Li, J.T.;, *et al*. T-BFA: Targeted bit-flip adversarial weight attack. IEEE Trans. Pattern Anal. Mach. Intell., **2022**, *44*: 7928−7939. doi: 10.1109/TPAMI.2021.3112932
18. Sh en, Y.F.; Song, W.Q.; Ji, H.R.;, *et al*. Improved belief propagation polar decoders with bit-flipping algorithms. IEEE Trans. Commun., **2020**, *68*: 6699−6713. doi: 10.1109/TCOMM.2020.3017656
19. Bernstein, A.; Steiglitz, K.; Hopcroft, J.. Encoding of analog signals for binary symmetric channels. IEEE Trans. Inf. Theory, **1966**, *12*: 425−430. doi: 10.1109/TIT.1966.1053921
20. Leung, H.; Seneviratne, C.; Xu, M. D.. A novel statistical model for distributed estimation in wireless sensor networks. IEEE Trans. Signal Process., **2015**, *63*: 3154−3164. doi: 10.1109/TSP.2015.2420536
21. Xi ao, J.J.; Cui, S.G.; Luo, Z.Q.;, *et al*. Power scheduling of universal decentralized estimation in sensor networks. IEEE Trans. Signal Process., **2006**, *54*: 413−422. doi: 10.1109/TSP.2005.861898
22. Xi ng, M.P.; Lu, J.Q.; Qiu, J.L.;, *et al*. Synchronization of complex dynamical networks subject to DoS attacks: An improved coding-decoding protocol. IEEE Trans. Cybern., **2023**, *53*: 102−113. doi: 10.1109/TCYB.2021.3090406
23. Di ng, J.; Sun, S.L.; Ma, J.;, *et al*. Fusion estimation for multi-sensor networked systems with packet loss compensation. Inf. Fusion, **2019**, *45*: 138−149. doi: 10.1016/j.inffus.2018.01.008
24. Ya ng, H.J.; Li, H.; Xia, Y.Q.;, *et al*. Distributed Kalman filtering over sensor networks with transmission delays. IEEE Trans. Cybern., **2021**, *51*: 5511−5521. doi: 10.1109/TCYB.2020.2980582
25. X in, D.J.; Shi, L. F.. Kalman filter for linear systems with unknown structural parameters. IEEE Trans. Circuits Syst. II: Express Briefs, **2022**, *69*: 1852−1856. doi: 10.1109/TCSII.2021.3103609
26. G e, Q.B.; Li, Y.Y.; Wang, Y.L.;, *et al*. Adaptive Kalman filtering based on model parameter ratios. IEEE Trans. Automat. Control, **2024**, *69*: 6230−6237. doi: 10.1109/TAC.2024.3376306
27. D ai, D.Y.; Li, J.H.; Song, Y.H.;, *et al*. Event-based recursive filtering for nonlinear bias-corrupted systems with amplify-and-forward relays. Syst. Sci. Control Eng., **2024**, *12*: 2332419. doi: 10.1080/21642583.2024.2332419
28. Wa ng, X.; Yaz, E. E.. Stochastically resilient extended Kalman filtering for discrete-time nonlinear systems with sensor failures. Int. J. Syst. Sci., **2014**, *45*: 1393−1401. doi: 10.1080/00207721.2013.879257
29. Abolmasoumi, A.H.; Farahani, A.; Mili, L.. Robust particle filter design with an application to power system state estimation. IEEE Trans. Power Syst., **2024**, *39*: 1810−1821. doi: 10.1109/TPWRS.2023.3263203
30. J in, Y.H.; Ma, X.S.; Meng, X.Y.;, *et al*. Distributed fusion filtering for cyber-physical systems under Round-Robin protocol: A mixed H_2/H_∞ framework. Int. J. Syst. Sci., **2023**, *54*: 1661−1675. doi: 10.1080/00207721.2023.2208130
31. L i, M.Q.; Chen, W.B.; Shao, Y.. Mixed H_∞-based finite-time passive filtering for a class of uncertain nonlinear singular systems. Optim. Control Appl. Methods, **2024**, *45*: 1122−1139. doi: 10.1002/oca.3092
32. Wa ng, F.; Liang, J. L.. Constrained H_∞ estimation for time-varying networks with hybrid incomplete information. Int. J. Robust Nonlinear Control, **2018**, *28*: 699−715. doi: 10.1002/rnc.3894
33. M a, L.F.; Wang, Z.D.; Lam, H.K.;, *et al*. Distributed event-based set-membership filtering for a class of nonlinear systems with sensor saturations over sensor networks. IEEE Trans. Cybern., **2017**, *47*: 3772−3783. doi: 10.1109/TCYB.2016.2582081
34. Sh en, Y.X.; Wang, Z.D.; Dong, H.L.;, *et al*. Set-membership state estimation for multirate nonlinear complex networks under FlexRay protocols: A neural-network-based approach. IEEE Trans. Neural Netw. Learn. Syst., **2025**, *36*: 4922−4933. doi: 10.1109/TNNLS.2024.3377537
35. H an, F.; Liu, J.H.; Li, J.H.;, *et al*. Consensus control for multi-rate multi-agent systems with fading measurements: The dynamic event-triggered case. Syst. Sci. Control Eng., **2023**, *11*: 2158959. doi: 10.1080/21642583.2022.2158959
36. Zh ou, J., A i, X. R.. Finite-time H_∞ filtering for Markov jump systems with partially unknown transition rates. Int. J. Adapt. Control Signal Process., **2024**, *38*: 3710−3730. doi: 10.1002/acs.3900
37. Zo ng, G.D.; Wang, R.H.; Zheng, W.X.;, *et al*. Finite-time H_∞ control for discrete-time switched nonlinear systems with time delay. Int. J. Robust Nonlinear Control, **2015**, *25*: 914−936. doi: 10.1002/rnc.3121

Citation: Ge, H.; Zou, L.; Chen, H.; *et al*. Finite-Time Bounded State Estimation for Time-Varying Systems Over FlexRay Networks With Probabilistic Bit Flips. *International Journal of Network Dynamics and Intelligence*. 2025, 4(4), 100023. doi: 10.53941/ijndi.2025.100023